Hybrid Precoding Based on Alternating Minimization for Millimeter Wave Systems

Mustafa Mulla

Submitted to the Institute of Graduate Studies and Research in partial fulfillment of the requirements for the degree of

Doctor of Philosophy in Electrical and Electronic Engineering

Eastern Mediterranean University May 2022 Gazimağusa, North Cyprus

Doctor of Philosophy in Electrical and Electronic Engineering. Assoc. Prof. Dr. Rasime Uyguroğlu Chair, Department of Electrical and Electronic Engineering We certify that we have read this thesis and that in our opinion it is fully adequate scope and quality as a thesis for the degree of Doctor of Philosophy in Electrical a Electronic Engineering. Prof. Dr. Ahmet Rizaner Co-Supervisor Prof. Dr. Ali Hakan Ulusoy Supervisor		
Chair, Department of Electrical and Electronic Engineering We certify that we have read this thesis and that in our opinion it is fully adequate scope and quality as a thesis for the degree of Doctor of Philosophy in Electrical a Electronic Engineering. Prof. Dr. Ahmet Rizaner Co-Supervisor Prof. Dr. Ali Hakan Ulusoy Supervisor Examining Committee		5
Chair, Department of Electrical and Electronic Engineering We certify that we have read this thesis and that in our opinion it is fully adequate scope and quality as a thesis for the degree of Doctor of Philosophy in Electrical a Electronic Engineering. Prof. Dr. Ahmet Rizaner Co-Supervisor Prof. Dr. Ali Hakan Ulusoy Supervisor Examining Committee	•	•
Prof. Dr. Ahmet Rizaner Co-Supervisor Prof. Dr. Ali Hakan Ulusoy Supervisor Examining Committee		Chair, Department of Electrical and
Co-Supervisor Supervisor Examining Committee		
	scope and quality as a thesis for the de	<u> </u>
1. Prof. Dr. Hasan Amca	scope and quality as a thesis for the de Electronic Engineering. Prof. Dr. Ahmet Rizaner	gree of Doctor of Philosophy in Electrical and Prof. Dr. Ali Hakan Ulusoy
	scope and quality as a thesis for the de Electronic Engineering. Prof. Dr. Ahmet Rizaner	gree of Doctor of Philosophy in Electrical and Prof. Dr. Ali Hakan Ulusoy
2. Prof. Dr. Mehmet Ertuğrul Çelebi	Prof. Dr. Ahmet Rizaner Co-Supervisor	Prof. Dr. Ali Hakan Ulusoy Supervisor
3. Prof. Dr. Aykut Hocanın	Prof. Dr. Ahmet Rizaner Co-Supervisor 1. Prof. Dr. Hasan Amca	Prof. Dr. Ali Hakan Ulusoy Supervisor
4. Prof. Dr. Erdal Panayırcı	Prof. Dr. Ahmet Rizaner Co-Supervisor 1. Prof. Dr. Hasan Amca 2. Prof. Dr. Mehmet Ertuğrul Çelebi	Prof. Dr. Ali Hakan Ulusoy Supervisor
5. Prof. Dr. Ali Hakan Ulusoy	Prof. Dr. Ahmet Rizaner Co-Supervisor 1. Prof. Dr. Hasan Amca 2. Prof. Dr. Mehmet Ertuğrul Çelebi	Prof. Dr. Ali Hakan Ulusoy Supervisor

ABSTRACT

Millimeter-wave frequencies, which enable the usage of a greater spectrum than the existing cellular microwave bands, have attracted the researchers' attention significantly. However, the ever-increasing demand for higher data rates in the future 5G and 6G networks requires further improvement of spectral efficiency. Millimeter-wave systems take advantage of the decrease in wavelength to employ antenna arrays consisting of a large number of antennas on both transmitter and the receiver. Due to the high hardware cost and high power consumption of the fully digital precoders used in conventional MIMO systems, it is not feasible to employ fully digital baseband precoders at the millimeter-wave MIMO systems. Hybrid analog/digital transceiver architectures, which were made up of digital baseband and analog RF precoders were recently proposed by many researchers to reduce the rather high power consumption. Since analog RF precoders are much cheaper and consume much lower powers, the cost of the system is also significantly reduced with the help of RF precoders while achieving a comparable fully-digital precoder performance.

This thesis investigates the performance of the millimeter-wave massive MIMO systems with hybrid analog/digital architecture for several aspects. We propose a novel low-complexity alternating minimization algorithm based on the Barzilai-Borwein (BB) gradient algorithm to maximize the spectral efficiency in single-user millimeter-wave systems under Gaussian noise and impulsive noise. It is aimed to minimize the Euclidean distance between the hybrid precoders and fully digital precoder using alternating minimization techniques for both scenarios. In the impulsive noise

environment, a novel fuzzy logic-based decoder is also proposed to suppress the effects of impulsive noise.

Simulation results demonstrate that the proposed BB method can achieve almost the same spectral efficiency as the competing methods despite its lower computational complexity. Furthermore, the proposed fuzzy logic-based filter successfully suppresses the impulsive noise effects and achieves a better bit error rate performance than the competing methods which also work efficiently in Gaussian noise.

Keywords: Millimeter-wave, massive MIMO, hybrid precoding, alternating minimization, BB gradient algorithm

Mevcut hücresel mikrodalga bantlarından daha geniş bir spektrumun kullanılmasını sağlayan milimetre-dalga frekansları, araştırmacıların dikkatini önemli ölçüde çekmiştir. Bununla birlikte, gelecekteki 5G ve 6G ağlarında daha yüksek veri hızlarına yönelik sürekli artan talep, spektral verimliliğin daha da iyileştirilmesini gerektiriyor. Milimetre-dalga sistemleri hem verici hem de alıcı üzerinde çok sayıda antenden oluşan anten dizilerini kullanmak için dalga boyundaki azalmadan yararlanır. Geleneksel MIMO sistemlerinde kullanılan dijital ön kodlayıcıların yüksek donanım maliyeti ve yüksek güç tüketimi nedeniyle, milimetre-dalga MIMO sistemlerinde dijital ön kodlayıcıların yalnız başına kullanılması uygun değildir. Bu yüzden, dijital ve analog RF ön kodlayıcılardan oluşan hibrit analog/dijital alıcı-verici sistemleri, son zamanlarda oldukça yükselen güç tüketimini azaltmak için birçok araştırmacı tarafından önerildi. Analog RF ön kodlayıcılar sayesinde sistem maliyeti ve güç tüketimi düşürülürken, dijital ön kodlayıcılara yakın bir performans elde edilmiştir.

Bu tez, hibrit analog/dijital yapıya sahip milimetre-dalga masif MIMO sistemlerinin performansını çeşitli açılardan incelemektedir. Tezde, tek kullanıcılı millimetre-dalga sistemlerinin Gauss gürültüsü ve anlık gürültü etkisi altında spektral verimliliğini en üst düzeye çıkarmak için düşük karmaşıklığa sahip Barzilai-Borwein (BB) gradyan algoritmasına dayanan özgün bir dönüşümlü minimizasyon algoritması önerilmiştir. Dönüşümlü minimizasyon teknikleri kullanılarak hibrit ön kodlayıcılar ile tam dijital ön kodlayıcı arasındaki Öklid mesafesinin en aza indirilmesi amaçlanmaktadır. Ayrıca, anlık gürültü ortamından kaynaklanan etkileri bastırmak için özgün bir bulanık mantık tabanlı kod çözücü önerilmiştir.

Simülasyon sonuçları, önerilen BB yönteminin daha düşük hesaplama karmaşıklığına

sahip olmasına rağmen, yarıştığı yöntemlerle neredeyse aynı spektral verimliliğe

ulaşabildiğini göstermektedir. Ayrıca, önerilen bulanık mantık tabanlı filtre, anlık

gürültü etkilerini başarıyla bastırırken kıyaslanan diğer yöntemlerden daha iyi bir hata

oranı elde etmiştir. Önerilen filtrenin, Gauss gürültüsü etkisi altında da yüksek

verimlilik ile çalıştığı gözlemlenmiştir.

Anahtar Kelimeler: Milimetre-dalga, masif MIMO, hibrit ön kodlayıcı, dönüşümlü

minimizasyon, BB gradyan algoritması

vi

DEDICATION

This dissertation is dedicated to my parents, wife, friends, and teachers who always support me during my journey in Ph. D. studies

ACKNOWLEDGEMENT

I would like to express my deepest gratitude to my supervisors, Prof. Dr. Ali Hakan Ulusoy and Prof. Dr. Ahmet Rizaner, for their constant guidance and endless support throughout my doctoral studies. This work would not be possible without their assistance and I am extremely thankful to them for believing in me.

A special thanks to Prof. Dr. Hasan Amca and Prof. Dr. Aykut Hocanin for their valuable contributions and suggestions to this project. They always ask me tough questions in the thesis monitoring meetings and help me find better solutions which eventually improve my work. I would also like to thank jury members Prof. Dr. Erdal Panayırcı and Prof. Dr. Mehmet Ertuğrul Çelebi for accepting our invitation and I am very honored to hear such good words from them.

Many thanks to all of my colleagues at EMU Electrical and Electronic Engineering for their encouragement and moral support, it was always fun to work with them. Also, I am indebted to my beloved friends for motivating and supporting me whenever I needed them, I am very lucky to have such friends.

Last, but not least, I am very grateful for my parent's unconditional and continuous support.

TABLE OF CONTENTS

ABSTRACT	iii
ÖZ	v
DEDICATION	vii
ACKNOWLEDGEMENT	viii
LIST OF TABLES	xii
LIST OF FIGURES	xiii
LIST OF SYMBOLS AND ABBREVIATIONS	xv
1 INTRODUCTION	1
1.1 Introduction	1
1.2 Thesis Aims and Objectives	3
1.3 Thesis Contribution	4
1.4 Publications	6
1.5 Thesis Outline	6
2 LITERATURE REVIEW	8
2.1 mmWave MIMO Systems	8
2.1.1 MIMO Architectures for mmWave Communications	8
2.1.1.1 Precoding Techniques	9
2.1.1.1 Analog Beamforming	10
2.1.1.1.2 Digital Precoding	11
2.1.1.3 Hybrid Analog/Digital Precoding	12
2.2 Minimization Methods for Hybrid Precoding	14
2.2.1 Orthogonal Matching Pursuit	15
2.2.2 Alternating Minimization	16

2.2.2.1 Orthogonal Procrustes Problem based Alternating Minimi	zation 16
2.2.2.2 Manifold Optimization-based Alternating Minimization	17
2.3 Impulsive Noise and Mitigation Techniques	20
3 SYSTEM MODEL AND PROBLEM FORMULATION	22
3.1 System Model for Single-User mmWave Hybrid Massive MIMO	22
3.1.1 Channel Model	24
3.2 Fuzzy Logic based Receiver for IN Mitigation	25
3.2.1 Impulsive Noise	26
3.2.1.1 Gaussian Mixture Model based on Middleton Class A	27
3.3 Problem Formulation for Hybrid Precoding	28
4 PROPOSED BARZILAI-BORWEIN ALGORITHM FOR HYBRID PRE	CODING
	31
4.1 Gradient Algorithms	31
4.1.1 Gradient Descent Method	33
4.1.2 Steepest Descent Method	34
4.1.3 Conjugate Gradient Method	35
4.2 Euclidean Barzilai-Borwein Gradient Algorithm	37
4.3 Riemannian Barzilai-Borwein Algorithm	39
4.4 Proposed Alternating Minizimiation Algorithm	41
4.4.1 Digital Baseband Precoder Design	42
4.4.2 Analog Precoder Design based on Riemannian BB Method	42
4.4.3 Two-Staged Hyrbid Precoder Design	43
4.4.4 Complexity Analysis	44
5 PROPOSED ADAPTIVE FUZZY LOGIC-BASED FILTER	46
5.1 Receiver Model for Impulsive Noise Environment	46

5.1.1 Fuzzy Median Filter Design	47
5.1.2 Threshold Mechanism to Detect Outlier Amplitudes	49
5.1.2.1 Z-Score Method to detect Outlier Amplitudes	49
5.1.2.2 Modified Z-Score to Detect Outlier Amplitudes	50
6 SIMULATION RESULTS	52
6.1 Simulation Results for GN Environment	53
6.2 Simulation Results for IN Environment	59
7 CONCLUSIONS AND FUTURE WORK	65
7.1 Conclusions	65
7.2 Future Work	67
REFERENCES	68

LIST OF TABLES

Table 4.1: Computational Cost of the Proposed and Competing Methods	44
Table 6.1: Improvement of Computational Cost of BB over CG	59
Table 6.2: Numerical Representation of the Computational Costs	59

LIST OF FIGURES

Figure 2.1: Analog beamforming architecture for single-user mmWave massive
MIMO
Figure 2.2: Digital precoding architecture for single-user mmWave massive MIMO.
Figure 2.3: Hybrid analog/digital precoding architecture for single-user mmWave
massive MIMO systems. 13
Figure 2.4: Analog beamforming schemes for hybrid precoding (a) fully connected
structure (b) sub-connected structure. 14
Figure 2.5: The illustration of manifold ${\mathcal M}$ with the tangent space and tangent vector
[26]
Figure 3.1: System model for hybrid analog/digital architecture in single-user
mmWave massive MIMO system23
Figure 3.2: Simplified hybrid receiver architecture with a fuzzy median filter for single
user mmWave massive MIMO system
Figure 5.1: Block diagram of the fuzzy median filter at the receiver
Figure 6.1: Spectral Efficiency versus SNR under GN
Figure 6.2: Spectral Efficiency versus the number of RF chains under GN
Figure 6.3: Coverage probability versus threshold values under GN
Figure 6.4: BER versus SNR under GN
Figure 6.5: (a) Spectral efficiency versus the number of BS antennas for $NMS = 36$,
and (b) the number of MS antennas for NBS = 144 under GN
Figure 6.6: (a) The number of mult. & div. versus the number of BS antennas, and (b)
the number of mult. & div. versus the number of RF chains

Figure 6.7: BER versus SNR in Gaussian channel ($\epsilon = 0$) for fuzzy filter with
threshold and without threshold
Figure 6.8: BER versus noise threshold in Gaussian channel ($\epsilon=0$) and IN channel
$(\epsilon = 0.02)$ (a) SNR = 6 dB (b) SNR = 20 dB60
Figure 6.9: BER versus SNR in IN channel (a) ($\epsilon = 0.02$), and (b) ($\epsilon = 0.04$) 62
Figure 6.10: BER versus epsilon for SNR values 5 dB, 10 dB, and 20 dB
Figure 6.11: Spectral efficiency versus SNR in IN channel (a) ($\epsilon = 0.02$), and ($\epsilon = 0.02$)
0.04)63

LIST OF SYMBOLS AND ABBREVIATIONS

|.| Absolute value

 $\| \cdot \|_F$ Frobenius norm

 $\langle \mathbf{a}_1, \mathbf{a}_2 \rangle$ Inner product of \mathbf{a}_1 and \mathbf{a}_2

• Element wise multiplication

 $\nabla f(.)$ Euclidean gradient of the cost function

⊗ Kronecker product

Pseudo-inverse

-1 Inverse

A Impulsive index

a_{BS} Antenna array response vector in the base station

 \mathbf{a}_{MS} Antenna array response vector in the mobile station

C Set of complex numbers

C Symmetric complex

d Space between antenna elements

det(.) Determinant of a matrix

D_{MF} Matched Filter linear digital precoder

D_{WF} Wiener Filter linear digital precoder

 \mathbf{D}_{ZF} Zero Forcing linear digital precoder

E[.] Expectation

exp(.) Exponential function

f(x) Objective function

f(x) Noise density function of Gaussian mixture model

 $f_A(x)$ Power density function of Middleton Class A

F_{BB} Digital baseband precoder

 $f_G(x)$ Noise density function for Gaussian background noise

F^I Imaginary part of fuzzifier

 $f_I(x)$ Noise density function with higher variance representing

impulsive noise components

F_{opt} Optimal fully digital precoder

 F^R Real part of fuzzifier

F_{RF} Analog RF precoder

grad Riemannian gradient of a function

H Channel matrix

Hermitian Hermitian

Im(.) Imaginary part of a vector or matrix

 I_N Identity matrix with the size $N \times N$

 \mathcal{M} Manifold

m Transmitted signal vector

M(k) Modified Z-score

 \mathcal{M}_{cc} Manifold on the complex circle

med(.) Median

med¹ Imaginary part of median

med^R Real part of median

min(.) Minimization

n Noise vector

N(.) Gaussian probability density function

 $N_{\rm BS}$ The number of base station antennas

 $N_{\rm cl}$ The number of clusters

 $N_{\rm MS}$ The number of mobile station antennas

 $N_{\rm ray}$ The number of rays

 $N_{\rm RF}$ The number of RF chains

 $N_{\rm s}$ The number of transmitted symbols

O(.) Time complexity

p and q Antenna indices

P(.) Coverage probability

 P_r Average received power for digital precoders

Proj_a Orthogonal projection on a

R Achievable rate (Spectral Efficiency)

 \mathbb{R} Set of real numbers

r Received signal vector

Re(.) Real part of a vector or matrix

Retr Retraction on \mathcal{M}_{cc}^{m}

 r^F Output of the fuzzy median filter

 r^{I} Imaginary part of the received signal after applying fuzzy filter

R_n Noise covariance matrix after decoding

 r^R Real part of received signal after applying fuzzy filter

s Transmitted symbol vector

std(.) Standard deviation

std^I Imaginary part of standard deviation

std^R Real part of standard deviation

T Sampling time

Transpose Transpose

Th Threshold

Tr(.) Trace of a matrix

 T_x Tangent space at a given point x

vec(.) Vectorization

W_{BB} Digital baseband decoder

W_{opt} Optimal fully digital decoder

 \mathbf{W}_{RF} Analog RF decoder

y The received signal vector after decoding

Z(k) Z-score

 α_{il} Complex gain of the *l*th ray in the *i*th cluster

 γ Curves through x

Γ The ratio of background Gaussian and non-Gaussian noise

 δ Channel normalization factor

 ε Occurrence probability

 η Termination criterion

 $\theta_{il}^{\mathrm{BS}}$ Elevation angle of departure

 θ_{il}^{MS} Elevation angle of arrival

 κ Impulsive noise variance factor

 λ Wave-length

 μ Mean

 ξ_x Tangent vector at a point x

 ρ Average received power of mmWave hybrid precoding system

 σ_n^2 Average noise power

 σ_w^2 Variance of Gaussian noise

 σ_z^2 Variance of impulsive noise

 ϕ_{ii}^{BS} Azimuth angle of departure

 ϕ_{il}^{MS} Azimuth angle of arrival

16-QAM Sixteen symbols-Quadrature Amplitude Modulation

3G 3rd Generation

4G 4th Generation

5G 5th Generation

6G 6th Generation

ADC Analog to Digital Converter

AWGN Additive White Gaussian Noise

BB Barzilai-Borwein

BER Bit Error Rate

BFGS Broyden-Fletcher-Goldfarb-Shanno

BS Base Station

CG Conjugate Gradient

DAC Digital to Analog Converter

dB Decibel

GD Gradient Descent

GHz Giga Hertz

GN Gaussian Noise

GP Gradient Projection

IN Impulsive Noise

LTE Long-Term Evolution

MAD Median Absolute Deviation

MIMO Multiple-Input-Multiple-Output

mmWave Millimeter wave

MO Manifold Optimization

MS Mobile Station

no. of mult. & div. The number of multiplications and divisions

OMP Orthogonal Matching Pursuit

OP Optimal Precoder

OPP Orthogonal Procrustes Problem

pdf Power density function

PF Penalty Function

QAM Quadrature Amplitude Modulation

RF Radio Frequency

RM Riemannian Manifold

SD Steepest Descent

SINR Signal to Impulsive Noise Ratio

SNR Signal to Noise Ratio

SQP Sequential Quadratic Programming

SVD Singular Value Decomposition

VLC Visible Light Communication

Chapter 1

INTRODUCTION

1.1 Introduction

Mobile broadband communication requires a significant expansion in the existing network capacity. Because of the dramatic growth in the number of users as a result of the increased demand for smart system applications, the network capacity should be increased to meet the demands of the users. According to the studies in this field, the traffic load is expected to increase by 1000 times in the next decade, and the current 4th Generation (4G) network will be insufficient to meet the huge demand [1], [2]. Thus, a new generation network called the 5th Generation (5G) needs to be employed for a new spectrum with much higher bandwidth. Millimeter-wave (mmWave) communication with the available spectrum between 3 GHz (λ =100 mm) and 300 GHz (λ =1 mm) is a promising candidate for achieving such higher bandwidths. The available frequency band on mmWave is higher than all of the licensed spectrum used by today's wireless communication systems [3]–[5].

The capacity of the system can be increased further by employing advanced antenna and diversity techniques, such as massive Multiple-Input-Multiple-Output (MIMO) [6], [7]. In the conventional MIMO, precoding is implemented at baseband using fully digital precoders. However, digital precoders require a dedicated Radio Frequency (RF) chain with the signal mixers and analog-to-digital converters for each antenna element, which enormously increases power consumption and system complexity.

Hence, the researchers proposed hybrid analog/digital precoding to reduce the power consumption and hardware cost of the system, since the hybrid precoders require a very small number of RF chains compared to the number of antenna elements used in massive MIMO [8], [9].

Recent research findings state that minimizing the Euclidian distance between hybrid precoders and the optimal precoder (fully digital precoder) will lead to maximize the spectral efficiency [8]. This problem can be handled as an optimization problem and the main goal is to optimize the hybrid precoders with low complexity and comparable performance to fully digital precoders. Existing works in the literature are mostly heavily complex or have constraints causing performance losses, making them infeasible for practical use. This thesis focuses on finding a better way to optimize the hybrid precoders considering a unit modulus constraint formed by analog phase shifters.

Alternating minimization methods are investigated to design the hybrid precoders and this approach performs very close to the full digital solution [10], [11]. However, there are still some handicaps that should be pointed out such as the complexity and the restriction of the methods. Therefore, in search of different optimization methods without any restriction and with an acceptable complexity, it is discovered that the Barzilai-Borwein (BB) gradient method based on manifold optimization can be a good candidate to serve those needs [12]–[14]. However, besides the advantages of mmWave, there are some handicaps in mmWave which is not well addressed, such as the suppression of impulsive noise.

The conventional mmWave systems are mostly designed to operate only for the Gaussian Noise (GN) model. In many physical channels, such as urban and indoor radio channels, the ambient noise is known through experimental measurements to be non-Gaussian. Hence, recent research findings state that a mixture noise model with additive Impulsive Noise (IN) is a more realistic approximation for mmWave channels. In this thesis, several mitigation techniques to suppress the IN are investigated and a fuzzy-logic-based decoder is designed to minimize the effects of the IN by ordering the samples based on fuzzy rank.

1.2 Thesis Aims and Objectives

In mmWave MIMO, optimizing the hybrid precoders to achieve a close performance to the fully digital precoders with low complexity is the key point for the upgoing research in this area. Power consumption and the hardware cost of the system can be reduced substantially using hybrid precoders rather than the fully digital precoders used in conventional MIMO systems. The main aim of this study is to maximize the spectral efficiency performance of the hybrid precoders to approach the performance of fully digital precoders while reducing the complexity of the system compared with the existing methods in the literature. In this regard, alternating minimization techniques are investigated and applied to the hybrid precoders for different setups.

In this study, an improved alternating minimization method is proposed to satisfy the following objectives:

- To optimize hybrid precoders in mmWave MIMO systems using alternating minimization techniques for single user GN and IN environments.
- 2) To maximize spectral efficiency performance of the hybrid precoders to maintain a close performance to fully digital precoders for each setup.

- 3) To reduce the computational complexity of the system without any restrictions.
- 4) To mitigate IN, while maximizing the spectral efficiency for single user mmWave MIMO systems.

1.3 Thesis Contribution

This study mainly focuses on optimizing the hybrid precoders to achieve an approximate performance to fully digital precoders while keeping the complexity of the system at an acceptable level for practical implementation.

In this thesis, we first proposed an improved alternating minimization based on the BB gradient method for a single-user mmWave MIMO system with hybrid transceiver architecture, where the noise is distributed as GN. The hybrid precoders are optimized by minimizing the Euclidian distance between the hybrid precoders and the digital precoders. Simulation results demonstrate that the proposed method can achieve identical spectral efficiency performance with the competing methods in the literature with lower computational complexity. It should also be noted that this method has no restrictions to degrade the performance of the system.

The main contributions of this study can be summarized as:

- a) A novel BB gradient-based alternating minimization method is investigated and compared with the existing methods concerning computational complexity and spectral efficiency.
- BB method is applied using manifold optimization and this allows us to use the
 BB method without any restrictions causing performance losses.

- c) It is shown that the proposed method has an identical spectral efficiency performance with the competing methods in the literature with comparable performance to fully digital precoders.
- d) The time complexities of several algorithms are derived and observed that the proposed algorithm requires less computational cost than the well-known conjugate gradient algorithm.

In the literature, the noise is generally modeled as GN and the effects of the IN are considered negligible. However, recent research findings state that the IN present at the mmWave frequencies degrade the performance of the system and there is a need for a more realistic model which includes the IN components. Therefore, we adapt a mixture noise model and develop a filter to reduce the severe effects of the IN. In the mmWave environment, there is limited research about the mixture noise model and how to eliminate the IN to enhance the system's performance. In this regard, we designed a hybrid decoder with a fuzzy logic filter to suppress the effects of IN. Although fuzzy-logic-based filters are used in the microwave environment, there is no implementation in the literature for the mmWave environment. Therefore, we adapt the fuzzy logic filter using a novel threshold mechanism and the results are very promising compared with the existing methods in the literature.

The main contributions of this study can be summarized as:

- a) The mixture noise model is used to represent the noise in the mmWave environment rather than the GN that is used in almost all the research papers.
- b) A novel fuzzy-logic-based decoder is designed to minimize the effect of IN by ordering the samples based on fuzzy rank.

c) A novel threshold mechanism is developed to detect IN components and this enables the system to suppress the IN components while also working efficiently in the Gaussian environment under different scenarios.

1.4 Publications

This thesis is based on the following original publications:

- M. Mulla, A. H. Ulusoy, A. Rizaner, and H. Amca, "Barzilai-Borwein Gradient Algorithm Based Alternating Minimization for Single User Millimeter Wave Systems," *IEEE Wirel. Commun. Lett.*, 2020, doi:10.1109/LWC.2019. 2960691.
- M. Mulla, M. Sohail, A. H. Ulusoy, R. Uyguroğlu, A. Rizaner, and H. Amca, "A Single User Millimeter Wave Massive MIMO System using Defected Ground Structure and Metasurface Antenna Arrays," in 2021 IEEE 29th Signal Processing and Communications Applications Conference (SIU), 2021, pp. 1-4, doi: 10.1109/SIU53274.2021.9477798.
- M. Mulla, A. Rizaner, and A. H. Ulusoy, "Fuzzy Logic Based Decoder for Single-User Millimeter Wave Systems Under Impulsive Noise," Wirel. Pers. Commun., 2021, doi: 10.1007/s11277-021-09435-7.

1.5 Thesis Outline

The rest of the thesis is organized as follows: Chapter 2 provides the preliminary and necessary definitions for mmWave MIMO systems and precoding schemes to eliminate the interference. A hybrid precoding scheme is introduced for mmWave systems and several optimization techniques are investigated to solve the hybrid precoding problem. Besides, IN characteristics and mitigation techniques in the literature are reviewed. Chapter 3 demonstrates the system model of the mmWave massive MIMO system and presents the channel model for the designed mmWave

system. Noise model for the IN channels and the simplified architecture of decoder with a fuzzy median filter to suppress IN are expressed. Moreover, the spectral efficiency expression is derived for the hybrid precoding system and the hybrid precoding problem is formulated.

In chapter 4, the proposed alternating minimization based on the Riemannian BB method to solve the hybrid precoding problem is summarized and several gradient methods are investigated to build the proposed algorithm. The computational cost of the proposed method is analyzed and the complexity of the proposed method is shown together with the competing methods. Chapter 5 presents the design of the proposed fuzzy logic-based filter to reduce the effects of the IN before passing through the hybrid decoders. Additionally, a novel threshold mechanism is developed to detect the outlier amplitudes considered as the IN samples in which the fuzzy median filter is only applied to the received signals with IN.

Chapter 6 illustrates the simulation results of the proposed Riemannian BB algorithm under GN and the fuzzy median filter under IN. The simulations are conducted for several setups and the results are discussed for different circumstances. Finally, Chapter 7 draws a conclusion for the research and gives suggestions for future works in this area.

Chapter 2

LITERATURE REVIEW

In this chapter, the preliminary and necessary definitions for mmWave MIMO systems are explained and the optimization techniques to solve the hybrid precoding problem in the literature are also reviewed. Moreover, brief information about the IN channel characteristics and IN mitigation techniques are given.

2.1 mmWave MIMO Systems

Multiple antenna techniques are well investigated by the researchers to apply in both transmitter and receiver for the wireless systems. It is shown that the MIMO systems enhance the transmission rate, link reliability, and coverage [6], [15], [16]. Therefore, MIMO systems are the most popular candidates to deliver needed data rates for mmWave communication [7]. This subsection reviews the MIMO architecture for mmWave communication and emerging techniques of the mmWave MIMO communication network.

2.1.1 MIMO Architectures for mmWave Communications

Although MIMO technology has been deployed and widely used in current commercial systems such as the 3rd Generation (3G) and Long-Term Evolution (LTE), these systems are considered as sub-6GHz and only support a small number of antennas (maximum eight elements). MmWave communication systems are expected to have much more antenna array elements due to the small wavelength characteristic. Antenna arrays can be built from 32 to 256 elements with the advantage of small physical size and this architecture is called massive MIMO [17]. Therefore, several

MIMO techniques are investigated in the literature to enhance the spectral efficiency performance of the system with a lower number of RF chains compared to antenna array size. One of the popular candidates for future wireless systems to achieve a higher spectral efficiency using a lower order modulation is spatial modulation [18]–[20] which is also taking attention for Visible Light Communication (VLC) that can be used in the 6th Generation (6G) [21]. Another powerful approach is to build a hybrid precoding scheme to handle a large number of antennas with lower power consumption by reducing the number of RF chains connected to the antennas.

The architecture of the MIMO in mmWave and microwave frequencies is different from each other. In conventional MIMO, fully digital precoders are used to apply signal processing and this scheme is not feasible for a large number of antenna elements. Thus, a better strategy is needed to employ precoding in mmWave massive MIMO architecture. In the next subsection, we review the precoding techniques for the conventional and massive MIMO systems.

2.1.1.1 Precoding Techniques

Precoders are designed to control the amplitude and phases of the transmitting signal to cancel the interference in advance to optimize mobile networks' performance. The use of precoding techniques has an important role in mmWave massive MIMO systems. In the literature, precoding is also known as beamforming which aims to transmit pencil-shaped beams to the selected terminals directly with no interference [22], [23]. There are three primary architecture schemes for precoding: analog beamforming, digital precoding, and hybrid analog/digital precoding. An overview of these schemes will be introduced in the following subsections.

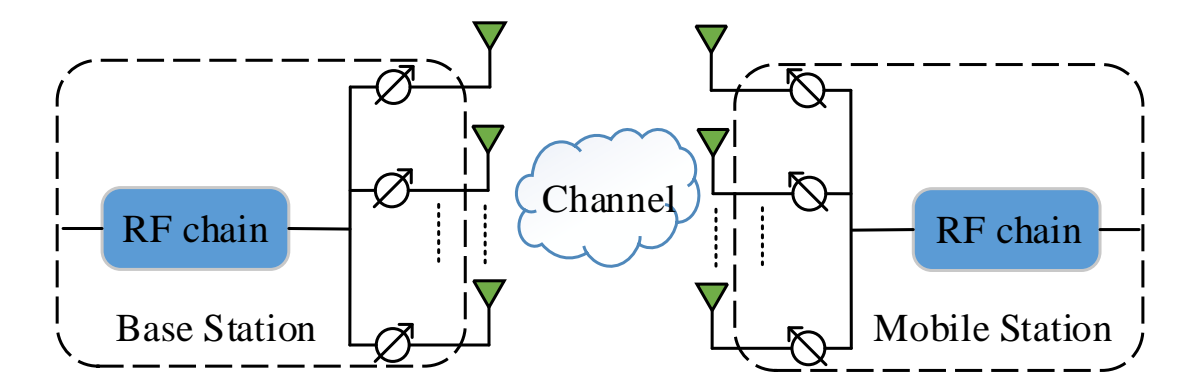


Figure 2.1: Analog beamforming architecture for single-user mmWave massive MIMO.

2.1.1.1 Analog Beamforming

Analog beamforming is one of the most basic methods to implement for mmWave MIMO systems, which can be used in both transmitter and receiver. Figure 2.1 illustrates the mmWave MIMO system using analog beamforming, where several antenna elements are attached to a single RF chain using simple phase shifters. In this approach, the phase of the signal is controlled with the network of digitally controlled phase shifters to achieve an optimal array gain and effective Signal to Noise Ratio (SNR) [17], [22].

Analog beamforming scheme requires a small number of RF chains compared with the large number of antenna elements used in mmWave massive MIMO. However, despite the simplicity of the hardware implementation, the performance of the analog beamforming scheme is poor due to the constant amplitude constraint of the design. Hence, fully digital precoding is preferable for low frequencies to eliminate the interference effects since both the amplitude and the phase can be controlled by the digital precoders for optimal performance [24].

2.1.1.1.2 Digital Precoding

Digital precoding is a conventional design for low-frequency applications in MIMO systems. It aims to eliminate interference in advance by controlling both the amplitude and the phase of the transmitting signal. Digital precoding can be classified under two categories as linear and nonlinear. Linear precoding schemes form the transmitted signal using a linear combination of the original signals and nonlinear precoders do this process in a nonlinear way.

Throughout this thesis, we will only focus on linear digital precoding schemes, including Matched Filter, Zero Forcing, and the Wiener Filter precoder, ordered in increasing depending on their complexities and performances. The system model for single-user mmWave massive MIMO system using fully digital precoding is shown in Figure 2.2, and to have a general understanding, the linear precoder models are derived respectively in (2.1) as:

$$\mathbf{D}_{MF} = \sqrt{\frac{M}{\operatorname{tr}(\mathbf{F}\mathbf{F}^{H})}}\mathbf{F}, \mathbf{F} = \mathbf{H}^{H}$$

$$\mathbf{D}_{ZF} = \sqrt{\frac{M}{\operatorname{tr}(\mathbf{F}\mathbf{F}^{H})}}\mathbf{F}, \mathbf{F} = \mathbf{H}^{H}(\mathbf{H}\mathbf{H}^{H})^{-1}$$

$$\mathbf{D}_{WF} = \sqrt{\frac{M}{\operatorname{tr}(\mathbf{F}\mathbf{F}^{H})}}\mathbf{F}, \mathbf{F} = \mathbf{H}^{H}\left(\mathbf{H}\mathbf{H}^{H} + \frac{\sigma_{n}^{2}M}{P_{r}}\mathbf{I}\right)^{-1},$$
(2.1)

where M denotes the transmitted number of data streams, \mathbf{H} represents the channel matrix between the transmitter and receiver, P_r and σ_n^2 denote the average received power and the noise power, respectively, and the corresponding linear digital precoders are referred as $\mathbf{D}_{MF,ZF,WF}$ [22].

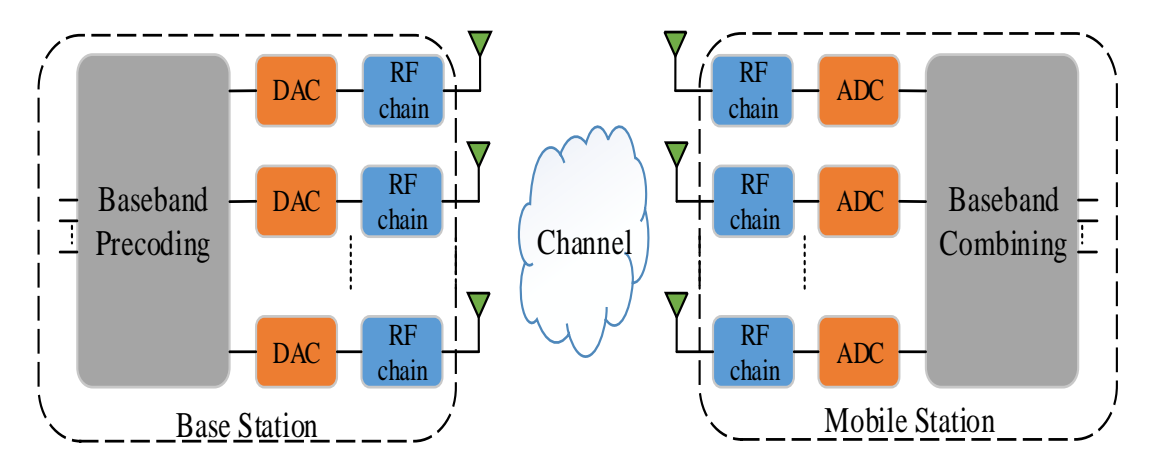


Figure 2.2: Digital precoding architecture for single-user mmWave massive MIMO.

At mmWave frequencies, there are several hardware limitations for using the fully digital precoding, and this makes the system infeasible in practice for a large number of antenna elements that are used in massive MIMO. A dedicated Analog to Digital Converter (ADC) / Digital to Analog Converter (DAC) and RF chain are required for each antenna element in digital precoding. This will increase the energy consumption and hardware cost enormously. Thus, hybrid analog/digital precoding technique is proposed to solve this problem [8] and the required number of RF chains is reduced while achieving a close performance to fully-digital precoders [22], [24].

2.1.1.1.3 Hybrid Analog/Digital Precoding

Hybrid analog/digital precoding scheme is a promising candidate for mmWave massive MIMO systems to overcome the challenges that occurred in analog and digital precoding schemes. This scheme is proposed to reduce the number of RF chains needed to employ fully digital precoding, which will significantly reduce energy consumption and hardware cost while achieving a near-optimal performance compared to digital precoding schemes. In hybrid precoding, the precoding process is divided into two domains as digital and analog domains. In the first step, a small-size digital precoder with a small number of RF chains is applied to eliminate the effects

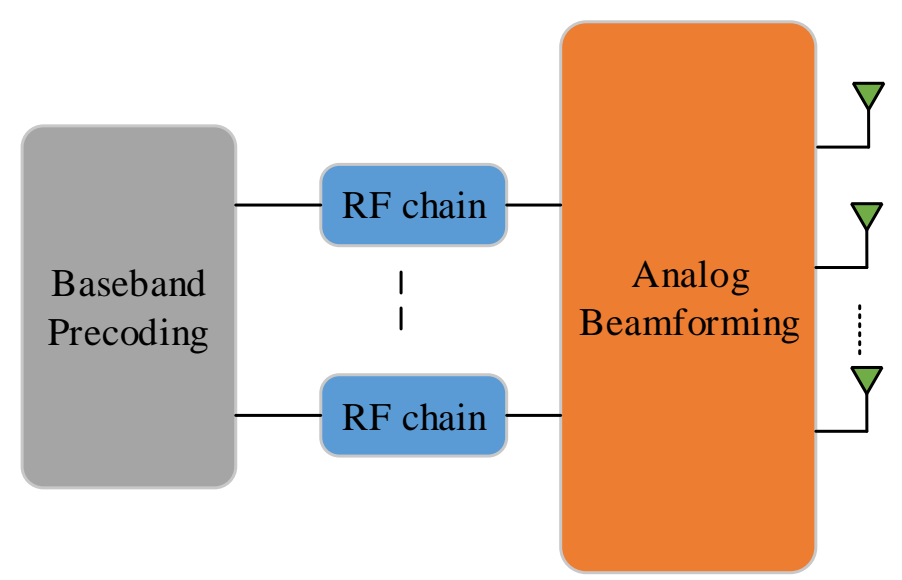


Figure 2.3: Hybrid analog/digital precoding architecture for single-user mmWave massive MIMO systems.

of interference, and antenna array gain is increased by employing a large-size analog beamformer using only phase shifters in the second step [7], [8], [17], [22], [24]. The system model for the mmWave massive MIMO with hybrid precoding is illustrated in Figure 2.3.

Hybrid precoders can be divided into two groups depending on their analog beamforming structure. Analog beamforming can be employed using different techniques such as phase shifters and switches. There are two main hybrid architectures: fully connected architecture, also known as spatially sparse precoding, and sub-connected architecture. In the first approach, all the antennas are connected to each RF chain using phase shifters, and in the second approach, antennas are divided into subgroups and all subgroups are connected to each RF chain [8], [17], [22], [24]—[26]. Two architectures for analog beamforming using phase shifters are shown in Figure 2.4.

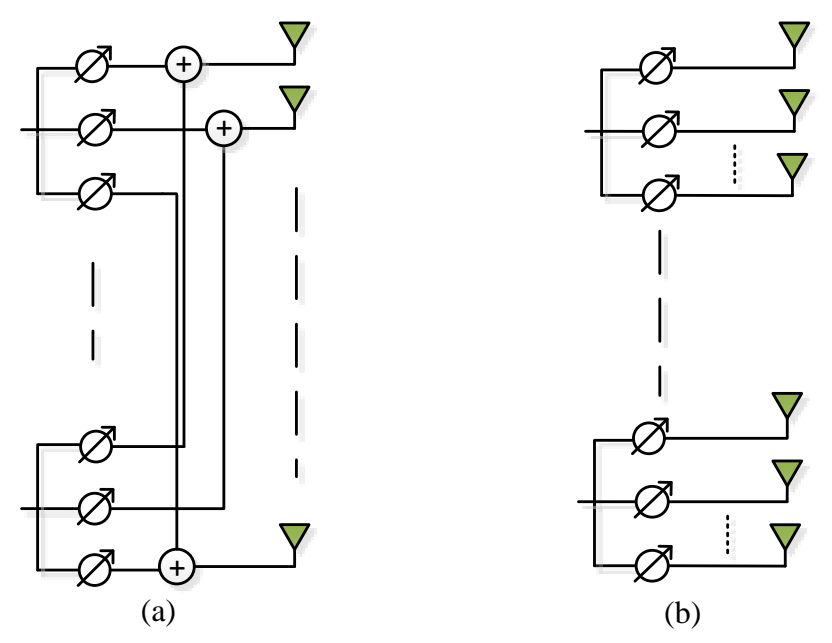


Figure 2.4: Analog beamforming schemes for hybrid precoding (a) fully connected structure (b) sub-connected structure.

In this thesis, we investigated hybrid precoding with a fully connected structure based on phase shifters, and the mathematical models for this structure are expressed in Chapter 3.

2.2 Minimization Methods for Hybrid Precoding

In recent years, research interest is growing rapidly on optimizing the hybrid precoders using minimization methods. Significant amounts of efforts have been invested in solving the hybrid precoding problem in mmWave massive MIMO systems to achieve a near-optimal spectral efficiency performance with low complexity compared with fully digital precoding. It is stated that minimizing the Euclidian distance between the hybrid precoders and optimal precoder (fully digital precoder) results in maximizing the spectral efficiency performance of the system [8]. In this subsection, the minimization techniques and alternating minimization methods in the literature will be investigated.

2.2.1 Orthogonal Matching Pursuit

In the literature, hybrid precoders are mostly designed using a fully connected structure and most of the works are based on Orthogonal Matching Pursuit (OMP), which achieves near-optimal performance. It is pointed out that the spectral efficiency can be maximized by optimizing the hybrid precoders using an algorithmic precoding solution based on OMP [8]. Optimal precoders are given as input to this algorithm and beam steering vectors are approximated to apply at RF. The columns of the RF precoding matrix are picked from the channel's array response vector and thus, hybrid precoding based on OMP can be considered a sparse matrix approximation problem. Although the complexity of the problem is reduced, there will be performance losses for feasible RF precoding solutions [8], [10], [27], [28].

An algorithmic solution based on OMP is presented in [8] and the hybrid precoder problem is solved using an optimization approach. The given algorithm first finds the channel's array response vector so that the optimal precoder achieves a maximum projection. After that, it aims to attach the selected array response vector onto the analog precoder and once the dominant vector is obtained, the digital precoder is computed using a direct least square approach. Finally, the residual precoding matrix is found by removing the selected vector and the digital precoder is normalized at the end of the algorithm to ensure the transmit power constraint.

In addition to performance losses, extra overhead is needed to obtain the information of array response vectors, and researchers are focused on reducing the computational cost of the OMP algorithm. Therefore, alternating minimization based hybrid precoding algorithms are proposed by the researchers and we review the alternating minimization methods for fully-connected structure in the next subsection.

2.2.2 Alternating Minimization

In mmWave MIMO, there is still a search to find a sophisticated method for solving the hybrid precoding problem with the unit modulus constraint. In this regard, alternating minimization algorithms are taking attention from the researchers, and several alternating minimization based algorithms are proposed. The main principle of alternating minimization is to divide the hybrid precoding problem into two subproblems, which are the analog and digital precoder design. It is aimed to optimize the digital precoder and analog precoder alternately to achieve near-optimal performance with an acceptable complexity [10], [11], [29]. In this subsection, several alternating minimization algorithms are investigated and the drawbacks and limitations of these algorithms are discussed to present a guideline for selecting the suitable alternating minimization method for the hybrid precoding problem.

2.2.2.1 Orthogonal Procrustes Problem based Alternating Minimization

Authors in [10] and [11] proposed an alternating minimization algorithm based on Orthogonal Procrustes Problem (OPP) to solve the hybrid precoding problem. The motivation of this algorithm is to acquire a low computational complexity with a slight performance loss compared with the algorithms in the literature. The Procrustes problem aims to approximate a matrix $\mathbf{A} \in \mathbb{R}^{m \times n}$ from a matrix $\mathbf{B} \in \mathbb{R}^{p \times n}$ multiplied by a matrix that has orthogonal columns $\mathbf{U} \in \mathbb{R}^{m \times p}$. Thus, the problem can be written using the Frobenius norm as

$$\min \|\mathbf{A} - \mathbf{U}\mathbf{B}\|_F^2 \text{ subject to } \mathbf{U}^T \mathbf{U} = \mathbf{I}_p. \tag{2.2}$$

The matrix **U** has orthonormal columns, therefore the Frobenius part of the equation (2.2) can be written as

$$\|\mathbf{A} - \mathbf{U}\mathbf{B}\|_F^2 = \text{Tr}(\mathbf{A}^T \mathbf{A}) - 2\text{Tr}(\mathbf{A}\mathbf{B}^T \mathbf{U}^T) + \text{Tr}(\mathbf{B}^T \mathbf{B}), \tag{2.3}$$

where minimizing (2.2) is equivalent to maximizing $Tr(\mathbf{AB}^T\mathbf{U}^T)$ and \mathbf{U} can be maximized using the Singular Value Decomposition (SVD) of \mathbf{AB}^T [30], [31].

Since the digital precoder satisfies the orthogonal property, the OPP algorithm can be applied to the hybrid precoding problem to determine the phases of the analog precoder with unit constraint from the equivalent precoder formed by the digital precoder and the optimal precoder [10], [11]. Although the OPP-based hybrid precoding algorithm requires low computational cost, this algorithm is not practical because of the restrictions. In the OPP algorithm, the number of transmitted symbols and RF chains should be equal to each other to achieve comparable spectral efficiency performance with the competing methods. Hence, in search of different optimization methods without any restrictions and with an acceptable complexity, it is discovered that the Manifold Optimation (MO) based alternating minimization can be a strong candidate to solve the hybrid precoding problem. In the next subsection, the fundamentals of the MO are reviewed to have a general understanding of the proposed BB alternating minimization algorithm based on MO, which will be discussed in detail in Chapter 4.

2.2.2.2 Manifold Optimization-based Alternating Minimization

The essential idea of this study is to find a method to solve the hybrid precoding problem without any restrictions and reduce the complexity of the competing methods in the literature. Thus, the MO-based algorithms are investigated and the authors in [10] proposed a MO-based alternating minimization algorithm for hybrid precoding. This method optimizes the analog precoders and digital precoders alternately while fixing the other. Since jointly optimizing these two matrices are highly complex due to the unit modulus constraint of the analog precoder, the solution requires two steps. In the first step, the digital precoder is solved with a fixed analog precoder using a

single least-square solution. In the second step, the analog precoder is optimized using Conjugate Gradient (CG) algorithm based on MO for fixed digital precoder.

In this subsection, the fundamentals and terminologies about the MO will be provided and our proposed Riemannian BB algorithm for analog precoding given in Chapter 4 will be built on this ground.

Manifold can be considered as a topological space that is locally similar to some Euclidean space with certain properties. The illustration of manifold \mathcal{M} is shown in Figure 2.5, where $T_x\mathcal{M}$ denotes the tangent space at a given point x on the manifold \mathcal{M} , and ξ_x and γ represent the tangent vector at a point x and the curves through x, respectively [10], [32], [33].

Riemannian Manifold (RM) is a special type of topological manifold that can be used for most applications. In this manifold, tangent space $T_x\mathcal{M}$ is equipped with a smoothly varying inner product that can be considered as Riemannian metric and this allows to use of calculus on the RM. Besides, the gradients of cost functions can be defined using the rich geometry of RM, and optimization techniques can be applied on the manifold over a Euclidian space without any constraints or smooth constraints [32]. In the hybrid precoding design, analog precoding vector deploys a complex circle manifold in which the complex plane \mathbb{C} with Euclidian metric can be represented as

$$\langle \mathbf{x}_1, \mathbf{x}_2 \rangle = \text{Re}\{\mathbf{x}_1^H \mathbf{x}_2\},\tag{2.4}$$

and the complex circle can be expressed as

$$\mathcal{M}_{cc} = \{ \mathbf{x} \in \mathbb{C} : \mathbf{x}^H \mathbf{x} = 1 \}. \tag{2.5}$$

Tangent vectors are used to characterize the directions of the movement for a given point x on the manifold \mathcal{M}_{cc} and thus, the tangent space can be specified as

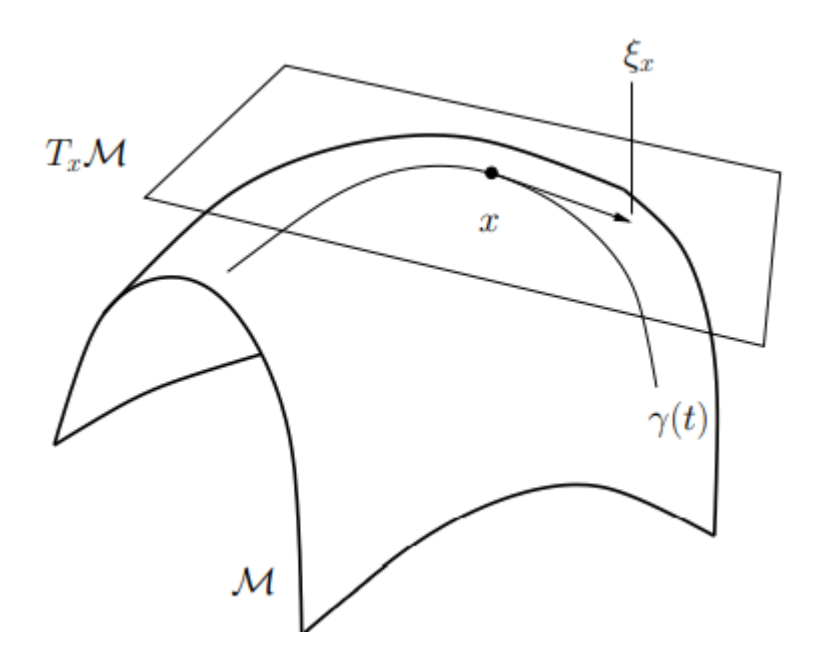


Figure 2.5: The illustration of manifold \mathcal{M} with the tangent space and tangent vector [32].

$$T_{\mathbf{x}}\mathcal{M}_{cc} = \{\mathbf{z} \in \mathbb{C} : \mathbf{z}^{H}\mathbf{x} + \mathbf{x}^{H}\mathbf{z} = 2\langle \mathbf{x}, \mathbf{z} \rangle = 0\},$$
(2.6)

where the analog precoding vector \mathbf{x} on the complex circle manifold is in the form

$$\mathcal{M}_{cc} = \{ \mathbf{x} \in \mathbb{C} : |\mathbf{x}_1| = |\mathbf{x}_2| = \dots = |\mathbf{x}_m| = 1 \},$$
 (2.7)

such that m is equal to the number of transmitting antennas times the number of RF chains. Hence, the optimization problem for analog precoding can be considered as a Riemannian submanifold of \mathbb{C}^m which has product geometry over m circles in the complex plane and the tangent space at $\mathbf{x} \in \mathcal{M}_{cc}^m$ can be defined as

$$T_{\mathbf{x}}\mathcal{M}_{cc}^{m} = \{\mathbf{z} \in \mathbb{C}^{m} : \operatorname{Re}\{\mathbf{z} \circ \mathbf{x}^{H}\} = \mathbf{0}_{m}\}, \tag{2.8}$$

where \circ denotes the elementwise multiplication. The direction of the maximum decrease of a function can be found using negative Riemannian gradient and the Riemannian gradient at \mathbf{x} is the orthogonal projection of the Euclidean gradient $\nabla f(\mathbf{x})$ along the tangent space $T_x \mathcal{M}_{cc}^m$ in which can be derived as

$$gradf(x) = Proj_{\mathbf{x}} \nabla f(\mathbf{x})$$

$$= \nabla f(\mathbf{x}) - Re{\nabla f(\mathbf{x}) \circ \mathbf{x}^{H}} \circ \mathbf{x},$$
(2.9)

where $\nabla f(\mathbf{x})$ is expressed in Chapter 4 [10], [32]. Based on the above terminology, the Riemannian BB algorithm [14] can be used to solve analog precoding problem and the details about this algorithm can be found in Chapter 4.

2.3 Impulsive Noise and Mitigation Techniques

Noise is commonly modeled using Gaussian distribution in the literature. On the other hand, the noise at the mmWave frequencies appears to be non-Gaussian and a mixed noise model with GN and IN can be used to express this noise model. The main source of IN is thought to be man-made and neighboring equipment frequently causes additive IN to the receivers. Since 5G technology needs an ultra-dense cellular network and the use of machine-to-machine communication is increasing day by day, the receivers are predicted to be impacted by a mixed noise rather than the traditional white GN defined in most of the studies. Furthermore, IN can be used to represent the atmospheric and solar static signals caused by the sunspots, which are likely to decrease the communication quality in mmWave bands [34], [35]. The Middleton class A model [36] is a widely accepted and realistic model to evaluate the mixture noise model for wireless communication channels [37]-[40], and it has been demonstrated that the presence of IN has a negative impact on systems performance for applications operating at mmWave frequencies [41]–[45]. Besides, the authors in [46] investigate the degradation of the performance of massive MIMO systems under IN. Thus, a sophisticated method should be developed to detect and mitigate the effects of IN in mmWave massive MIMO systems.

Several detectors have been designed to improve the performance of the systems under the effects of IN, and the majority of the works are based on clipping and blanking [47]–[49]. Although these methods are straightforward to apply, the Bit Error Rate (BER) performances of the systems are insufficient for practical use in mmWave. The authors in [50] proposed a threshold mechanism is for detecting impulses, and the performance of the system is improved by using an optimal threshold. The system's performance, however, is still poor for practical use, and a more sophisticated method is required. Additionally, to increase the performance of IN filters, neural networks and deep learning algorithms are expressed [51]–[53].

The fuzzy logic-based algorithm presented in [54] is another effective strategy to mitigate IN and it has been discovered that this statistical method can meet our objectives. This method aims to organize the samples with fuzzy order and then reduce the effects of IN using a fuzzy median filter. For IN channels, this approach works well, but the performance is expected to degrade when the noise is distributed as Gaussian. Therefore, to detect the impulses, a threshold mechanism is designed in [55] and a fixed threshold is set to ensure the system to work in both impulsive and Gaussian scenarios.

An adaptive threshold mechanism is implemented in [56] to enhance the system's performance further and the filter is only applied to the identified impulses. Statistical metrics, median, and standard deviation are used to choose the optimal threshold adaptively for each received signal. It is indicated here that the threshold applied performance of the system in the Gaussian environment is much better than the system without any threshold.

Chapter 3

SYSTEM MODEL AND PROBLEM FORMULATION

In this chapter, first, the system model for single-user mmWave massive MIMO and channel model for the considered system are presented. Then, IN characteristics and simplified architecture of fuzzy logic-based decoder to mitigate IN are introduced. Finally, the hybrid precoding problem is formulated, and mathematical formulations are expressed.

3.1 System Model for Single-User mmWave Hybrid Massive MIMO

The system model for a single-user mmWave hybrid massive MIMO system is shown in Figure 3.1. This research focused on the downlink model, where $N_{\rm S}$ symbols are transmitted by the Base Station (BS) using $N_{\rm BS}$ transmit antennas and received by a single Mobile Station (MS) operating with $N_{\rm MS}$ receive antennas. The number of RF chains are denoted as $N_{\rm RF}$ and for simplicity, it is assumed that both the BS and MS have the same number of $N_{\rm RF}$ with the constraint $N_{\rm S} \leq N_{\rm RF} \leq N_{\rm BS}$, $N_{\rm MS}$.

The transmitted signal vector $\mathbf{m} \in \mathbb{C}^{N_{\mathrm{BS}} \times 1}$ can be written as

$$\mathbf{m} = \mathbf{F}_{RF} \mathbf{F}_{BB} \mathbf{s},\tag{3.1}$$

where $\mathbf{s} \in \mathbb{C}^{N_{\mathrm{S}} \times 1}$ denotes the transmitted symbol vector normalized by

$$\mathbb{E}[\mathbf{s}\mathbf{s}^H] = \frac{1}{N_s}\mathbf{I}_{N_s}.\tag{3.2}$$

The hybrid precoders are the combination of digital baseband precoder $\mathbf{F}_{BB} \in \mathbb{C}^{N_{RF} \times N_S}$ and analog RF precoder $\mathbf{F}_{RF} \in \mathbb{C}^{N_{BS} \times N_{RF}}$ in which normalized to satisfy the power constraint as

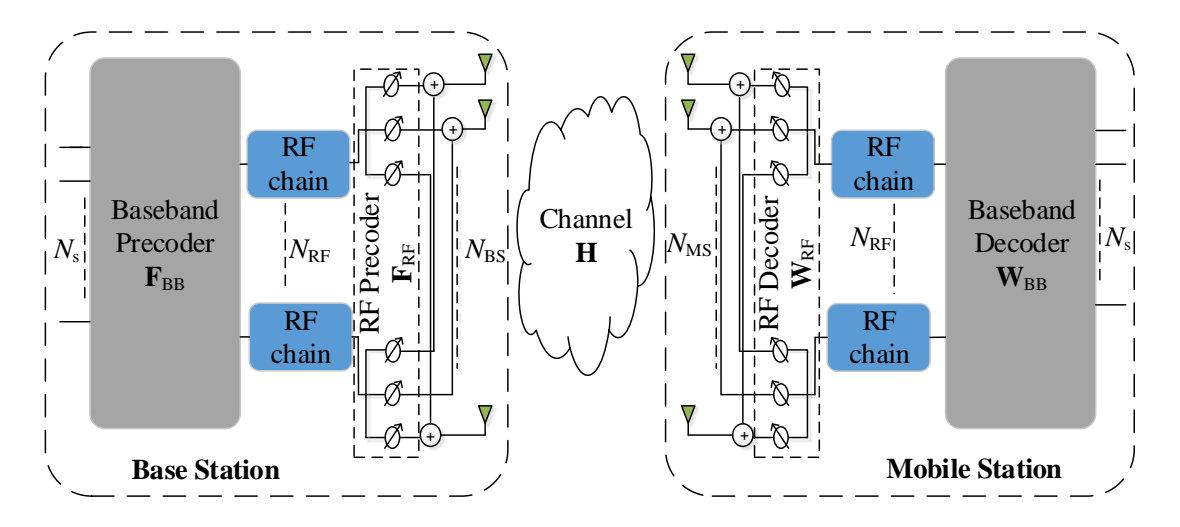


Figure 3.1: System model for hybrid analog/digital architecture in single-user mmWave massive MIMO system.

$$\|\mathbf{F}_{RF}\mathbf{F}_{BB}\|_F^2 = N_{s}.\tag{3.3}$$

Hence the received signal vector $\mathbf{r} \in \mathbb{C}^{N_{\text{MS}} \times 1}$ observed by the MS can be formulated as

$$\mathbf{r} = \sqrt{\rho} \mathbf{H} \mathbf{F}_{RF} \mathbf{F}_{BB} \mathbf{s} + \mathbf{n}, \tag{3.4}$$

where ρ denotes the average received power, $\mathbf{H} \in \mathbb{C}^{N_{\mathrm{MS}} \times N_{\mathrm{BS}}}$ refers to the channel matrix between the BS and the MS, and $\mathbf{n} \in \mathbb{C}^{N_{\mathrm{MS}} \times 1}$ represents the noise vector. The noise vector is expressed using two different models. In the first model, the noise vector \mathbf{n} is distributed using circularly symmetric complex Gaussian definition with zero mean and covariance matrix $\sigma^2 \mathbf{I}_{N_{\mathrm{MS}}}$ in the form:

$$\mathbf{n} \sim \mathcal{C}N(0, \sigma^2 \mathbf{I}_{N_{\rm MS}}),\tag{3.5}$$

and in the second model, \mathbf{n} is defined using the Gaussian mixture model that is explained in the next subsection [8], [10], [11], [29], [57], [58].

At the receiver, the received signal \mathbf{r} is decoded using the hybrid decoders, which consist digital baseband decoder $\mathbf{W}_{BB} \in \mathbb{C}^{N_{RF} \times N_S}$ and analog RF decoder $\mathbf{W}_{RF} \in \mathbb{C}^{N_{MS} \times N_{RF}}$. Thus, the received signal after decoding operation can be expressed as

$$\mathbf{y} = \sqrt{\rho} \mathbf{W}_{BB}^{H} \mathbf{W}_{RF}^{H} \mathbf{H} \mathbf{F}_{RF} \mathbf{F}_{BB} \mathbf{s} + \mathbf{W}_{BB}^{H} \mathbf{W}_{RF}^{H} \mathbf{n}, \tag{3.6}$$

where the RF precoders and decoders are designed to perform only using phase shifters and they can only manipulate the phase of the signals. Therefore, the magnitude of all nonzero elements are equal and have unit modulus constraint shown as [10], [11], [29]

$$\left| (\mathbf{F}_{RF})_{i,k} \right| = \left| (\mathbf{W}_{RF})_{i,k} \right| = 1. \tag{3.7}$$

3.1.1 Channel Model

Multipath models for lower frequency can be used to express mmWave channels [59]; however, the highly directional nature of propagation at mmWave makes the beamspace representation more suitable [60]. Besides, mmWave channels have sparse channel characteristics due to the high space path loss and limited scattering [61], [62]. Thus, in this thesis, Saleh-Valenzuela [63] clustered channel model is used to express the representation of narrowband mmWave channels [64]–[66], and the channel matrix **H** can be evaluated as

$$\mathbf{H} = \sqrt{\frac{N_{\rm BS}N_{\rm MS}}{N_{\rm cl}N_{\rm ray}}} \sum_{i=1}^{N_{\rm cl}} \sum_{l=1}^{N_{\rm ray}} \alpha_{il} \left[\mathbf{a}_{\rm MS} (\boldsymbol{\phi}_{il}^{\rm MS}, \boldsymbol{\theta}_{il}^{\rm MS}) \, \mathbf{a}_{\rm BS} (\boldsymbol{\phi}_{il}^{\rm BS}, \boldsymbol{\theta}_{il}^{\rm BS})^H \right], \tag{3.8}$$

where $N_{\rm cl}$ and $N_{\rm ray}$ represent the number of clusters and number of rays respectively, $lpha_{il}$ denotes the complex channel gain of the lth ray in the ith cluster. It is assumed that the α_{il} has independent and identical (i.i.d) distribution that is given by

$$\alpha_{il} \sim \mathcal{C}N(0, \sigma^2 \mathbf{I}),$$
 (3.9)

in which normalized by a factor

$$\sum_{i=1}^{N_{\rm cl}} \sigma^2 \mathbf{I} = \delta \tag{3.10}$$

to ensure the channel power constraint

$$\mathbb{E}[\|\mathbf{H}\|_F^2] = N_{\rm BS} N_{\rm MS}. \tag{3.11}$$

In addition, $\mathbf{a}_{MS}(\phi_{il}^{MS}, \theta_{il}^{MS})$ and $\mathbf{a}_{BS}(\phi_{il}^{BS}, \theta_{il}^{BS})$ represent the antenna array response vectors in the MS and BS, respectively, while the azimuth (elevation) angles of arrival and departures are denoted as the coefficients $\phi_{il}^{MS}(\theta_{il}^{MS})$ and $\phi_{il}^{BS}(\theta_{il}^{BS})$. The array geometry is assumed as a uniform square planar array and under this consideration, the array response vector at the BS can be defined as

$$\mathbf{a}_{\rm BS}(\phi_{il}^{\rm BS}, \theta_{il}^{\rm BS}) = \frac{1}{\sqrt{N_{\rm BS}}} \begin{bmatrix} 1, \dots, e^{j\frac{2\pi}{\lambda}d} (p\sin(\phi_{il}^{\rm BS})\sin(\theta_{il}^{\rm BS}) + q\cos(\theta_{il}^{\rm BS}), \\ \dots, e^{j(\sqrt{N_{BS}} - 1)\frac{2\pi}{\lambda}d} (\sin(\phi_{il}^{\rm BS})\sin(\theta_{il}^{\rm BS}) + \cos(\theta_{il}^{\rm BS})) \end{bmatrix}^T, \quad (3.12)$$

where λ and d represent the wavelength of the signal and the space between antenna elements respectively, and p and q indicate the indices of the antennas such that, $0 \le p \le \sqrt{N_{\rm BS}}$ and $0 \le q \le \sqrt{N_{\rm BS}}$. The array response vector at the MS $\mathbf{a}_{\rm MS}(\phi_{il}^{\rm MS}, \theta_{il}^{\rm MS})$ can be defined using the same definition [10], [11], [57], [58], [66].

3.2 Fuzzy Logic based Receiver for IN Mitigation

Figure 3.2 illustrates the simplified hybrid receiver architecture with a fuzzy median filter to mitigate the IN in mmWave channels. In conventional mmWave hybrid decoding systems, the ambient noise is assumed to be AWGN and the effect of the noise is reduced using only the hybrid decoders as shown in Figure 3.1. However, for the IN environment, the IN components should be suppressed before passing the received signal through the decoder to avoid the enhancement of the IN level. Therefore, a fuzzy median filter is designed and attached to the hybrid decoder to minimize the effects of outlier amplitudes which is considered as IN. More information about the fuzzy median filter and the detailed schematic of the fuzzy algorithm is given in Chapter 5. Besides, the IN characteristics and the Gaussian mixture model based on Middleton Class A noise to express the IN behavior are introduced in the next subsection.

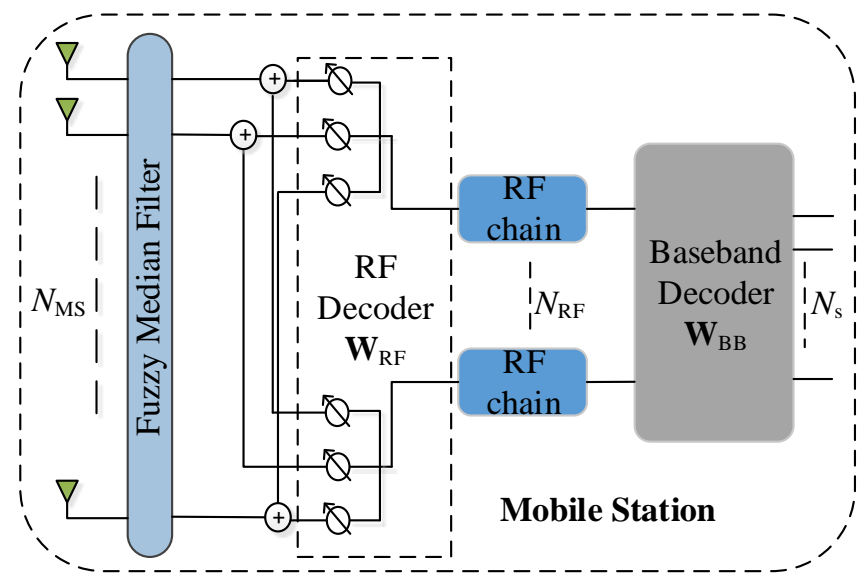


Figure 3.2: Simplified hybrid receiver architecture with a fuzzy median filter for single user mmWave massive MIMO system.

3.2.1 Impulsive Noise

In wireless communication, noise can affect the system in various ways depending on the source. In general, Gaussian distribution has been used to model the noise at the receiver of communication systems which is supported by the central limit theorem. On the other hand, it is shown that the ambient noise in various physical channels may have non-Gaussian behavior such as IN.

IN is made up of sudden sharp bursts which is a "on/off" sequence of random pulses in the time domain. The main source of IN is considered man-made and nearby devices often cause additive IN to the receivers. Since 5G technology requires an ultra-dense cellular network and machine-to-machine communication is growing rapidly, the receivers are expected to be affected by a mixed noise rather than the classical white GN expressed in most research papers. In addition, atmospheric and solar static signals caused by the sunspots and thunderstorms can also be represented by IN, and it is expected to degrade the communication quality in mmWave bands [34], [35], [67], [68].

3.2.1.1 Gaussian Mixture Model based on Middleton Class A

The nonlinearity of the electromagnetic interference is expressed by D. Middleton, considering the Gaussian component to represent the thermal noise at the receiver of communication systems. To evaluate the canonical description of several non-Gaussian behaviors in different environments, Middleton Class A, B, and C statistical noise models are presented [69], [70]. Middleton Class A model has been widely used in communication systems to represent the electromagnetic interference and the power density function (pdf) of this model can be shown as

$$f_A(x) = e^{-A} \sum_{n=0}^{\infty} \frac{A^n}{n! \sqrt{2\pi\sigma_n^2}} e^{\frac{-x^2}{2\sigma_n^2}},$$
 (3.13)

where $A \ge 0$ denotes the impulsive index, $\sigma_n^2 \ge 0$ represents the power of the noise that can be derived as $\left(\frac{n}{A} + \Gamma\right)/(1 + \Gamma)$, such that $\Gamma \ge 0$ is the ratio of the powers of background Gaussian and non-Gaussian noise components [71], [72].

The Gaussian mixture model is a two-term model to illustrate the behavior of non-Gaussian environments with the noise density function

$$f(x) = (1 - \varepsilon)f_G(x) + \varepsilon f_I(x) \tag{3.14}$$

where $0 \le \varepsilon \le 1$ denotes the mixture parameter, adjusting the occurrence probabilities of the two zero-mean Gaussian distributed probability density functions, $f_G(x)$ and $f_I(x)$, with different variance values [73], [74].

In this thesis, the behavior of IN is characterized using the Gaussian mixture model given by (3.14), which is an approximation of Middleton Class A noise. The Gaussian distributed noise components in the mixture are defined as $f_G(x) \sim N(0, \sigma_w^2)$ and $f_I(x) \sim N(0, \kappa \sigma_z^2)$, where σ_w^2 and $\kappa \sigma_z^2$ represent the variances of the mixture

components in (3.14), with $\kappa \geq 1$. Note that the variance of the IN depends on the level of Signal to Impulsive Noise Ratio (SINR) [36], [55], [56], [75]. Consequently, it is expected that the IN has severe impacts on mmWave channels and the mixture model adapted in (3.14) will be more realistic to indicate the behavior of the noise signal in the system [50].

3.3 Problem Formulation for Hybrid Precoding

The main goal of this thesis is to design the hybrid precoders, \mathbf{F}_{RF} and \mathbf{F}_{BB} , and the hybrid decoders, \mathbf{W}_{RF} and \mathbf{W}_{BB} , to maximize the achievable spectral efficiency. The spectral efficiency R for the hybrid precoding system given in Figure 3.1 can be derived as [8], [10], [11], [76]

$$R = \log_2 \det \left(\mathbf{I}_{N_s} + \frac{\rho}{N_s} \mathbf{R}_n^{-1} \mathbf{W}_{BB}^H \mathbf{W}_{RF}^H \mathbf{H} \mathbf{F}_{RF} \mathbf{F}_{BB} \mathbf{F}_{BB}^H \mathbf{F}_{RF}^H \mathbf{H}^H (\mathbf{W}_{RF} \mathbf{W}_{BB}) \right), \quad (3.15)$$

where \mathbf{R}_n denotes the noise covariance matrix after decoding that can be defined as

$$\mathbf{R}_n = \sigma_n^2 \mathbf{W}_{\mathrm{BB}}^H \mathbf{W}_{\mathrm{RF}}^H \mathbf{W}_{\mathrm{RF}} \mathbf{W}_{\mathrm{BB}}. \tag{3.16}$$

Since optimizing the problem as a joint problem with hybrid precoder and decoder together is too complex, the design of transmitter and receiver are handled separately as proposed in [8]. To simplify the maximizing problem of the spectral efficiency, the main problem is decoupled into two subproblems, and it is shown that the decoupled solution performs almost identical with the performance of a fully digital precoder/decoder that can be considered as the optimal solution. Both precoding and decoding problems have similar constraints and can be derived using the same mathematical expressions. Therefore, throughout this thesis, we will focus on the precoder design and the same approach will be applied to the decoder [8], [10], [11], [27].

After some mathematical approximations shown in [8], the hybrid precoding problem can be approached as an optimization problem and the problem is translated to design \mathbf{F}_{RF} and \mathbf{F}_{BB} that can be formulated as

$$\min_{\mathbf{F}_{RF}, \mathbf{F}_{BB}} \left\| \mathbf{F}_{\text{opt}} - \mathbf{F}_{RF} \mathbf{F}_{BB} \right\|_{F}^{2}$$
subject to $((\mathbf{F}_{RF})_{i,l}) \in \{\mathbf{a}_{BS}(\phi_{il}^{BS}, \theta_{il}^{BS}), \text{ for all } i, l\},$

$$\|\mathbf{F}_{RF} \mathbf{F}_{BB}\|_{F}^{2} = N_{S},$$
(3.17)

where \mathbf{F}_{opt} is referred for the optimal fully digital precoder. It has been pointed out that, minimizing the objective function (3.17) results to maximize the spectral efficiency [8], [10], [77].

Furthermore, the optimal precoder \mathbf{F}_{opt} and optimal decoder \mathbf{W}_{opt} can be approximated from the singular value decomposition of the channel matrix

$$\mathbf{H} = \mathbf{U} \mathbf{\Sigma} \mathbf{V}^H. \tag{3.18}$$

By considering, there are no hardware limitations and all the streams have equal power allocations, the first N_s columns of \mathbf{U} and \mathbf{V} maximize the data rates which are related with the highest singular values in Σ . Thus, the optimal precoder \mathbf{F}_{opt} and optimal decoder \mathbf{W}_{opt} can be obtained by the first N_s columns of the \mathbf{V} and \mathbf{U} , respectively [8], [11]. Hence, $\mathbf{F}_{\text{opt}} \in \mathbb{C}^{N_{\text{BS}} \times N_s}$ and $\mathbf{W}_{\text{opt}} \in \mathbb{C}^{N_{\text{MS}} \times N_s}$ can be approximated as [77], [78]

$$\mathbf{F}_{\text{opt}} \triangleq \mathbf{V}(:, 1: N_{\text{s}}) \text{ and } \mathbf{W}_{\text{opt}} \triangleq \mathbf{U}(:, 1: N_{\text{s}}),$$
 (3.19)

which also satisfy the following constraints similar to (3.17)

$$\|\mathbf{F}_{\text{opt}}\|_{F}^{2} = N_{\text{s}} \text{ and } \|\mathbf{W}_{\text{opt}}\|_{F}^{2} = N_{\text{s}}.$$
 (3.20)

Besides, optimal precoders and decoders have a semi-unitary structure that can be justified as [11]

$$\mathbf{F}_{\text{opt}}^H \mathbf{F}_{\text{opt}} = \mathbf{I}_{N_s} \text{ and } \mathbf{W}_{\text{opt}}^H \mathbf{W}_{\text{opt}} = \mathbf{I}_{N_s}.$$
 (3.21)

In this thesis, we propose a low complexity alternating minimization algorithm to solve the objective function (3.17). It is aimed to maximize the spectral efficiency and achieve a near-optimal performance that is close to a fully digital precoder which is defined as \mathbf{F}_{opt} . The problem will be considered as a matrix factorization problem with matrix variables \mathbf{F}_{RF} and \mathbf{F}_{BB} , and alternating minimization will be applied to this problem. Many researchers get attention to alternating minimization since this method can be applied for several optimization problems and achieves a near-optimal performance with different subsets of variables [79]–[83].

In [9] and [10], several alternating minimization algorithms for hybrid precoding problem are investigated and the results are very promising. Therefore, our research mainly focuses on solving the (3.17) using an alternating minimization method to achieve low computational cost with a very close spectral efficiency performance compared with the competing methods in the literature. The proposed method based on Riemannian BB is discussed in Chapter 4, and since jointly optimizing the hybrid precoders \mathbf{F}_{RF} and \mathbf{F}_{BB} is heavily complex, the problem is decoupled into two subproblems. Two matrices are optimized alternately while fixing the other, and this will be the main idea throughout this thesis.

Chapter 4

PROPOSED BARZILAI-BORWEIN ALGORITHM FOR HYBRID PRECODING

The work presented in this chapter is inspired by the alternating minimization methods to solve the hybrid precoding problem given in (3.17). In the first stage, the digital precoder \mathbf{F}_{BB} is solved using a direct least square approach by fixing the analog precoder \mathbf{F}_{RF} and in the second stage, analog precoder \mathbf{F}_{RF} is calculated using optimization techniques by fixing \mathbf{F}_{BB} . To find a nearly optimal solution for \mathbf{F}_{RF} , several gradient algorithms are investigated, and it is discovered that the BB gradient algorithm [12] can be applied to reduce the computational cost of the well-known CG algorithm.

In this chapter, first brief information about the gradient algorithms and conjugate gradient algorithm are given. After that, the conventional Euclidian BB [12] gradient algorithm is discussed, and to ensure the global convergence, Riemannian BB [14] algorithm is presented. Finally, the two-staged proposed alternating minimization algorithm for the hybrid precoder design is illustrated and the complexity of the proposed algorithm is analyzed.

4.1 Gradient Algorithms

This section summarizes the gradient algorithms to solve the analog precoder problem of the alternating minimization algorithm for hybrid precoder design. Several

algorithms are developed and their performances are compared to give us a direction to built our proposed algorithm. Consider a system of linear equations

$$\mathbf{A}\mathbf{x} = \mathbf{b},\tag{4.1}$$

where $\mathbf{A} \in \mathbb{C}^{n \times n}$ is a positive definite complex symmetric matrix, vector $\mathbf{b} \in \mathbb{C}^n$, and \mathbf{x} denotes the solution that we want to achieve. Thus, the problem given in (4.1) is the same as solving the unconstrainted optimization problem [84]

$$\min_{\mathbf{x} \in \mathbb{C}^n} (4.2)$$

where $f(\mathbf{x})$ can be written as

$$f(\mathbf{x}) = \frac{1}{2}\mathbf{x}^T \mathbf{A} \mathbf{x} - \mathbf{x}^T \mathbf{b}.$$
 (4.3)

The $f(\mathbf{x})$ is convex and the gradient of the cost function can be expressed as

$$\nabla f(\mathbf{x}) = \mathbf{A}\mathbf{x} - \mathbf{b}.\tag{4.4}$$

We will investigate the gradient algorithms to solve (4.2) in the following subsections. First, Gradient Descent (GD) and Steepest Descent (SD) algorithms are evaluated. However, these algorithms converge very slow and have high computational complexity for real-time implementation of hybrid precoder design. Besides, these algorithms have no global convergence guarantee and it is highly possible to get stuck in a local minimum while searching for a solution set. This leads us to find a better algorithm and we found out that the CG algorithm can serve better for our needs. Research findings prove that the CG has a higher convergence speed when compared with the competing gradient algorithms. However, the CG algorithm is still highly complex for practical use since it requires finding the search direction for every iteration. Therefore, the BB gradient algorithm is examined in the next section to reduce the computational cost of the well-known CG algorithm.

4.1.1 Gradient Descent Method

In the GD method, a negative gradient is selected as the search direction and the approximate minimizer is updated iteratively by the following equation

$$\mathbf{x}_{i+1} = \mathbf{x}_i - \alpha_i \mathbf{g}_i, \tag{4.5}$$

where α_i represents the step size, and \mathbf{g}_i denotes the gradient of the cost function

$$\mathbf{g}_i = \nabla f(\mathbf{x}_i),\tag{4.6}$$

The negative gradient is used to move toward the local minimum that is stated as

$$f(\mathbf{x}_{i+1}) < f(\mathbf{x}_i). \tag{4.7}$$

Besides, the step size α_i is selected in every iteration using a backtracking line search [85]. In the backtracking line search, the α_i starts with unit step size and then will be reduced by a factor 0.5 until it satisfies the following Armijo-Goldstein condition

$$f(\mathbf{x}_i - \alpha_i \mathbf{g}_i) \le f(\mathbf{x}_i) - \tau \alpha_i \nabla f(\mathbf{x}_i)^T \mathbf{g}_i, \tag{4.8}$$

where τ is chosen as 0.5 [84]–[87]. The summary for the GD method is given in Algorithm 1 [85] and η represents the termination criterion in all the algorithms.

Algorithm 1 Gradient Descent Method

Input: \mathbf{A} , \mathbf{b} and $\mathbf{x}_0 = \mathbf{b}$

- 1. Set i = 0, and calculate $\mathbf{g}_0 = \nabla f(\mathbf{x}_0)$
- 2. while $\|{\bf g}_i\|_2 > \eta$
- 3. Using the backtracking line search to find the step size α_i satisfying (4.8).
- 4. Update the solution $\mathbf{x}_{i+1} = \mathbf{x}_i \alpha_i \mathbf{g}_i$.
- 5. Calculate the gradient $\mathbf{g}_{i+1} = \nabla f(\mathbf{x}_{i+1})$.
- 6. i = i + 1
- 7. **end**

4.1.2 Steepest Descent Method

Although the GD method is a straightforward algorithm, the convergence rate is not good enough. Therefore, the SD method with an exact line search can be used to solve (4.2) to speed up the convergence rate. Since this is also a gradient method, the same approximate minimizer as shown in (4.5) is used in this algorithm. The step size α_i can be chosen using an exact line search as

$$\alpha_i = \frac{\mathbf{g}_i^T \mathbf{g}_i}{\mathbf{g}_i^T \mathbf{A} \mathbf{g}_i}.$$
 (4.9)

The SD method is summarized in Algorithm 2 [84], and a slight improvement in the convergence speed is observed compared to GD.

Algorithm 2 Steepest Descent Method

Input: \mathbf{A} , \mathbf{b} and $\mathbf{x}_0 = \mathbf{b}$

- 1. Set i = 0, and calculate $\mathbf{g}_0 = \nabla f(\mathbf{x}_0)$
- 2. while $\|{\bf g}_i\|_2 > \eta$
- 3. Find the step size using an exact line search as $\alpha_i = \frac{\mathbf{g}_i^T \mathbf{g}_i}{\mathbf{g}_i^T A \mathbf{g}_i}$.
- 4. Update the solution $\mathbf{x}_{i+1} = \mathbf{x}_i \alpha_i \mathbf{g}_i$.
- 5. Calculate the gradient $\mathbf{g}_{i+1} = \nabla f(\mathbf{x}_{i+1})$.
- 6. i = i + 1
- 7. **end**

In both Algorithm 1 and Algorithm 2, the matrix **A** should be extremely well-conditioned to have a reasonable convergence rate and to ensure global convergence. However, these algorithms are not preferable for practical use due to the slow convergence and there is a probability of converging into a local minimum rather than the global minimum [84], [85]. Thus, CG as a more sophisticated method is

investigated and it is proven that the convergence rate is much better than the other two gradient algorithms and it is known as global convergent [84], [86], [87].

4.1.3 Conjugate Gradient Method

The CG is a very efficient method since it requires much fewer iterations than the other descent algorithms to converge a critical point that can be considered the global minimum. In this section, the CG algorithm developed by Hestenes and Stieffel [88] is discussed to solve the optimization problem given in (4.2). The method starts with an initialization phase to compute the residual \mathbf{r}_0 , and direction vector \mathbf{p}_0 which can be obtained by the formula

$$\mathbf{p}_0 = \mathbf{r}_0 = \mathbf{b} - \mathbf{A}\mathbf{x}_0. \tag{4.10}$$

Then, the direction vector can be computed as

$$\mathbf{p}_{i+1} = \mathbf{r}_{i+1} + \delta_i \mathbf{p}_i, \tag{4.11}$$

where

$$\mathbf{r}_{i+1} = \mathbf{r}_i - \alpha_i \mathbf{A} \mathbf{p}_i \text{ and } \delta_i = \frac{\mathbf{r}_{i+1}^T \mathbf{r}_{i+1}}{\mathbf{r}_i^T \mathbf{r}_i}.$$
 (4.12)

Besides, the step size α_i is given by

$$\alpha_i = \frac{\mathbf{r}_i^T \mathbf{r}_i}{\mathbf{p}_i^T \mathbf{A} \mathbf{p}_i}.$$
 (4.13)

Finally, the approximate solution can be estimated as

$$\mathbf{x}_{i+1} = \mathbf{x}_i + \alpha_i \mathbf{p}_i. \tag{4.14}$$

It should be noted that the residuals are mutually orthogonal and direction vectors are mutually conjugate, such that

$$\langle \mathbf{r}_i, \mathbf{r}_j \rangle = 0 \text{ and } \langle \mathbf{p}_i, \mathbf{A}\mathbf{p}_j \rangle = 0 \text{ for } i \neq j.$$
 (4.15)

The summary of the CG is given in Algorithm 3 [84] and the computational cost of this algorithm will be presented in section 4.4.

Algorithm 3 Conjugate Gradient Method

Input: \mathbf{A} , \mathbf{b} and $\mathbf{x}_0 = \mathbf{b}$

- $1. \mathbf{p}_0 = \mathbf{r}_0 = \mathbf{b} \mathbf{A}\mathbf{x}_0$
- 2. **while** $\|\mathbf{r}_i\|_2 > \eta$
- 3. Determine the step size $\alpha_i = \frac{\mathbf{r}_i^T \mathbf{r}_i}{\mathbf{p}_i^T \mathbf{A} \mathbf{p}_i}$.
- 4. Compute the residual $\mathbf{r}_{i+1} = \mathbf{r}_i \alpha_i \mathbf{A} \mathbf{p}_i$ and then the coefficient $\delta_i = \frac{\mathbf{r}_{i+1}^T \mathbf{r}_{i+1}}{\mathbf{r}_i^T \mathbf{r}_i}$.
- 5. Compute the direction vector $\mathbf{p}_{i+1} = \mathbf{r}_{i+1} + \delta_i \mathbf{p}_i$.
- 6. Update the solution $\mathbf{x}_{i+1} = \mathbf{x}_i + \alpha_i \mathbf{p}_i$.
- 7. i = i + 1
- 8. **end**

The CG method is a very efficient and robust tool to solve the optimization problem defined in (4.2). However, it is still highly complex for practical implementation due to the computation of search direction for each iteration. Therefore, the conventional Euclidain BB gradient algorithm presented in [12] is investigated to reduce the computational cost. Research findings state that the conventional BB algorithm is not global convergent and the global convergence of the BB algorithm is proved for the Riemannian optimization on the special case of Stiefel manifolds [89]. The authors in [14] proposed a BB algorithm defined over RM and this algorithm can be used to solve the optimization problem of analog precoder by ensuring the global convergence while reducing the complexity of CG.

In the next section, the conventional Euclidean BB gradient algorithm is discussed to have a general understanding of the BB gradient method and then the Riemannian BB method is illustrated to solve the analog part of the alternating minimization problem.

4.2 Euclidean Barzilai-Borwein Gradient Algorithm

From the above discussions, it is known that the GD and SD methods have poor performance, slow convergence and conditioning plays an important role in their performance. Besides, CG performs almost perfectly with the help of a good convergence rate, but also this method is still highly complex and it is required to reduce the computation cost of the CG algorithm. In this regard, Barzilai and Borwein [12] developed a two-step size gradient method which is known as the BB gradient method and in this thesis, we called this method the Euclidean BB method.

Euclidean BB method is also a gradient method and aims to solve the problem in (4.2) considering the quadratic function (4.3). Therefore, the approximate minimizer has the same form as the GD as shown in (4.5) and the gradient of the cost function can be denoted as \mathbf{g}_i , same as (4.6).

In this method, the step size α_i is approximated using the secant equation in quasi-Newton methods. The Hessian approximation of f at \mathbf{x}_i is denoted as the matrix

$$\mathbf{D}_i = \alpha_i^{-1} \mathbf{I},\tag{4.16}$$

to satisfy the quasi-Newton property, such that

$$\min \|\mathbf{D}_{i+1}\mathbf{s}_i - \mathbf{y}_i\|. \tag{4.17}$$

Hence, the step size α_i is chosen as

$$\alpha_{i+1} = \frac{\mathbf{s}_i^T \mathbf{s}_i}{\mathbf{s}_i^T \mathbf{y}_i}. (4.18)$$

The α_i is derived from the information obtained at the points \mathbf{x}_i and \mathbf{x}_{i+1} , and thus, the \mathbf{s}_i and \mathbf{y}_i can be expressed as [12], [13], [90]–[92]

$$\mathbf{s}_i = \mathbf{x}_{i+1} - \mathbf{x}_i \text{ and } \mathbf{y}_i = \mathbf{g}_{i+1} - \mathbf{g}_i.$$
 (4.19)

Based on the above descriptions, the Euclidian BB algorithm can be summarized as shown in Algorithm 4 [12].

As it can be seen in Algorithm 4, there are no matrix calculations in the BB method, and the line search is only required for the initial condition i = 0. Since there is no need to find search directions for every iteration like the other gradient methods, this reduces the computational cost and greatly speeds up the convergence speed of the algorithm [13], [91]. However, there is no guarantee for the global convergence of the Euclidian BB method and there is a possibility to converge into a local minimum point. Therefore, the researchers in [14] have adapted a RM optimization to the problem, and the BB method's global convergence is ensured. In the next section, the background information about the Riemannian BB method will be given and the analog precoder part of the proposed alternating minimization algorithm will be optimized based on this adaptation.

Algorithm 4 Euclidian Barzilai-Borwein Gradient Method

Input: A, b and $\mathbf{x}_0 = \mathbf{b}$

- 1. Set i = 0, and calculate $\mathbf{g}_0 = \nabla f(\mathbf{x}_0)$ and find the step size α_0 by Armijo backtracking line search that satisfies (4.8).
- 2. **while** $\|\mathbf{g}_i\|_2 > \eta$
- 3. Update the solution $\mathbf{x}_{i+1} = \mathbf{x}_i \alpha_i \mathbf{g}_i$.
- 4. Calculate $\mathbf{g}_{i+1} = \nabla f(\mathbf{x}_{i+1})$.
- 5. Calculate \mathbf{s}_i and \mathbf{y}_i using (4.19)
- 6. Set α_{i+1} using (4.18)
- 7. i = i + 1
- 8. **end**

4.3 Riemannian Barzilai-Borwein Algorithm

Globally convergent BB methods are taking attention from the researchers to solve the optimization problem in (4.2), which is defined in Euclidean space. Euclidean BB algorithms are mostly preferred for their simplicity and low computational cost for each iteration. Besides, the performance of the practical implementation is nearly optimal for a good choice of step size [14], [91], [93]. However, the global convergence of the BB methods for different setups has always been a problem for researchers.

The authors in [94] proved the global convergence of the BB method for strictly convex quadratic functions, on the other hand, the property is not guaranteed for the nonquadratic case if there is no globalization strategy [95]. Since the cost function has a nonmonotone behavior due to the BB steps, the decrease condition for the cost function is generally not efficient at each step and the strategy becomes to set the cost functions to repeat maximum N steps. Research findings state that the convergence rate of the BB method does not change for large N values, which will make the BB method a good candidate to compete with CG [95], [96].

To generalize the global convergence of the BB method defined in the Euclidian space, a more general setting is considered in [14] and RM optimization is adapted to the problem. Thus, the cost function is defined over the RM \mathcal{M}_{cc}^m in which $\mathbf{x} \in \mathcal{M}_{cc}^m$ and the optimization problem can be stated as

$$\min_{\mathbf{x}} f(\mathbf{x}) \\
\mathbf{x} \in \mathcal{M}_{cc}^{m}.$$
(4.20)

In numerical optimization, iterative algorithms aim to compute a descent direction using the negative gradient of the objective function f(x) for a given point x and move

in the direction of the negative gradient until found a moderate decrease in f. In manifold optimization, the concept of moving along a tangent vector without leaving the manifold is called retraction and retraction can be used to map a vector from the tangent space to the manifold [32]. Therefore, the approximate minimizer on the manifold is modified as

$$\mathbf{x}_{i+1} = \text{Retr}_{\mathbf{x}_i}(-\alpha_i \mathbf{g}_i), \tag{4.21}$$

where Retr denotes the retraction on \mathcal{M}^m_{cc} and can be defined as [10]

$$Retr_{\mathbf{x}_i}(-\alpha_i \mathbf{g}_i) = vec \left[\frac{(\mathbf{x}_i - \alpha_i \mathbf{g}_i)}{|\mathbf{x}_i - \alpha_i \mathbf{g}_i|} \right], \tag{4.22}$$

where vec(.) represents the vectorization. Besides, the vectors \mathbf{s}_i and \mathbf{y}_i are modified for the adaptation of the RM. The increment $\mathbf{x}_{i+1} - \mathbf{x}_i$ is updated as

$$\mathbf{\tau}_i = -\alpha_i \mathbf{g}_i, \tag{4.23}$$

that belongs to the tangent space $T_{\mathbf{x}_i}\mathcal{M}_{cc}^m$ and it is transported to $T_{\mathbf{x}_{i+1}}\mathcal{M}_{cc}^m$ [14]. The vectors \mathbf{s}_i and \mathbf{y}_i require the operations from different tangent spaces which can be handled by mapping two tangent vectors from different tangent spaces. In this regard, the transport of gradient from \mathbf{x}_i to \mathbf{x}_{i+1} can be stated as [10]

$$T_{\mathbf{x}_{i} \to \mathbf{x}_{i+1}}(\mathbf{g}_{i}) = \mathbf{g}_{i} - \text{Re}\{\mathbf{g}_{i} \circ \mathbf{x}_{i+1}^{H}\} \circ \mathbf{x}_{i+1},$$
 (4.24)

and the modified \mathbf{s}_i can be specified as

$$\mathbf{s}_i = T_{\mathbf{\tau}_i}(\mathbf{\tau}_i) = T_{\mathbf{x}_i \to \mathbf{x}_{i+1}}(-\alpha_i \mathbf{g}_i) = -\alpha_i T_{\mathbf{x}_i \to \mathbf{x}_{i+1}}(\mathbf{g}_i). \tag{4.25}$$

Then \mathbf{y}_i is computed by subtracting two gradients from two different tangent spaces and the updated equation can be written as

$$\mathbf{y}_{i} = \mathbf{g}_{i+1} - T_{\mathbf{x}_{i} \to \mathbf{x}_{i+1}}(\mathbf{g}_{i}) = \mathbf{g}_{i+1} + \frac{1}{\alpha_{i}} T_{\tau_{i}}(\tau_{i}). \tag{4.26}$$

Finally, the step size for the Riemannian BB method is chosen as [14]

$$\alpha_{i+1} = \frac{\langle \mathbf{s}_i, \mathbf{s}_i \rangle_{\mathbf{x}_{i+1}}}{\langle \mathbf{s}_i, \mathbf{y}_i \rangle_{\mathbf{x}_{i+1}}}.$$
(4.27)

Based on the above descriptions, the summary for the Riemannian BB algorithm to solve the analog precoding problem is given in Algorithm 5 [14]. Brief information about the matrix manifolds can be found in Chapter 2, and more details about the manifold optimization can be found in [32].

This section summarizes the Riemannian BB method that will be used to solve the second stage of the proposed alternating minimization algorithm. In the second stage, \mathbf{F}_{RF} will be optimized using Algorithm 5 and the following section will introduce the proposed two-staged alternating minimization method to solve the objective function (3.17).

Algorithm 5 Riemannian Barzilai-Borwein Gradient Method [14]

Input: \mathbf{F}_{opt} , \mathbf{F}_{BB} and $\mathbf{x}_0 \in \mathcal{M}_{cc}^m$

- 1. Set i = 0, and calculate $\mathbf{g}_0 = \operatorname{grad} f(\mathbf{x}_0)$ and find the step size α_0 by Armijo backtracking line search that satisfies (4.8).
- 2. while $\|{\bf g}_i\|_2 > \eta$
- 3. Calculate $\mathbf{x}_{i+1} = \text{Retr}_{\mathbf{x}_i}(-\alpha_i \mathbf{g}_i)$ and $\mathbf{g}_{i+1} = \text{grad } f(\mathbf{x}_{i+1})$ using (2.9).
- 4. Calculate \mathbf{s}_i and \mathbf{y}_i using (4.25) and (4.26), respectively.
- 5. Set α_{i+1} using (4.27)
- 6. i = i + 1
- 7. **end**

4.4 Proposed Alternating Minizimiation Algorithm

The proposed algorithm is made up of two stages to solve (3.17), where digital precoder \mathbf{F}_{BB} and analog precoder \mathbf{F}_{RF} are alternately achieved with the principle of alternating minimization by fixing the other. Digital precoder \mathbf{F}_{BB} is obtained with a direct least square approach, while the Riemannian BB algorithm is used to optimize the analog precoder \mathbf{F}_{RF} .

4.4.1 Digital Baseband Precoder Design

In the first stage, the digital precoder \mathbf{F}_{BB} is obtained with a fixed analog precoder \mathbf{F}_{RF} . Hence, the problem (3.17) for the \mathbf{F}_{BB} design can be rewritten as

$$\min_{\mathbf{F}_{BB}} \left\| \mathbf{F}_{\text{opt}} - \mathbf{F}_{RF} \mathbf{F}_{BB} \right\|_{F}^{2}. \tag{4.28}$$

This equation can be solved by using a well-known least square solution as

$$\mathbf{F}_{\mathrm{BB}} = \mathbf{F}_{\mathrm{RF}}^{\dagger} \mathbf{F}_{\mathrm{BB}},\tag{4.29}$$

where the term $\mathbf{F}_{RF}^{\dagger}$ denotes the pseudo-inverse of the analog precoder that can be expressed as [10]

$$\mathbf{F}_{RF}^{\dagger} = (\mathbf{F}_{RF}^{H} \mathbf{F}_{RF})^{-1} \mathbf{F}_{RF}^{H} \mathbf{F}_{\text{opt}}.$$
 (4.30)

4.4.2 Analog Precoder Design based on Riemannian BB Method

In the second stage, analog precoder \mathbf{F}_{RF} can be optimized similarly with a fixed \mathbf{F}_{BB} considering the unit modulus constraint $|(\mathbf{F}_{RF})_{i,k}| = 1$. Thus, the analog precoder can be optimized using the following problem

$$\min_{\mathbf{F}_{RF}} \left\| \mathbf{F}_{\text{opt}} - \mathbf{F}_{RF} \mathbf{F}_{BB} \right\|_{F}^{2}, \tag{4.31}$$

where Algorithm 5 is applied to the problem to find a nearly optimal solution of the \mathbf{F}_{RF} . In the algorithm, the desired solution vector \mathbf{x} is denoted as [10], [11]

$$\mathbf{x} = \text{vec}(\mathbf{F}_{RF}). \tag{4.32}$$

Besides, the Euclidian gradient of the cost function in (4.31) can be derived as

$$\nabla f(\mathbf{x}) = -2(\mathbf{F}_{BB}^{H} \otimes \mathbf{I}_{N_{BS}}) \left[\operatorname{vec}(\mathbf{F}_{opt}) - (\mathbf{F}_{BB}^{H} \otimes \mathbf{I}_{N_{BS}}) \mathbf{x} \right], \tag{4.33}$$

where \otimes denotes the Kronecker product which is used to vectorize the second term of (4.31), $\text{vec}(\mathbf{x}\mathbf{F}_{BB})$ [97].

4.4.3 Two-Staged Hyrbid Precoder Design

The proposed alternating minimization algorithm is developed with the help of the above descriptions, and the Riemannian BB method shown in Algorithm 5. Hybrid precoder is designed to solve the problems (4.28) and (4.31) in two stages iteratively. The digital precoder \mathbf{F}_{BB} is normalized at the end of the algorithm to satisfy the power constraint of (3.17) and the normalization can be shown as

$$\widehat{\mathbf{F}_{\mathrm{BB}}} = \frac{\sqrt{N_{\mathrm{s}}}}{\|\mathbf{F}_{\mathrm{RF}}\mathbf{F}_{\mathrm{BB}}\|_{F}} \mathbf{F}_{\mathrm{BB}}.$$
(4.34)

The proposed alternating minimization algorithm based on the Riemannian BB method is shown in Algorithm 6.

Algorithm 6 Riemannian BB Based Alternating Minimization Algorithm for Hybrid Precoding

Input: F_{opt}

- 1. Set i = 0, and initialize $\mathbf{F}_{RF}(0)$ with random phases.
- 2. while (termination criterion $\geq \eta$)
- 3. Calculate $\mathbf{F}_{BB}(i) = \mathbf{F}_{RF}^{\dagger}(i)\mathbf{F}_{BB}(i)$ for a fixed $\mathbf{F}_{RF}(i)$.
- 4. For a fixed $\mathbf{F}_{BB}(i)$, optimize $\mathbf{F}_{RF}(i+1)$ by using Algorithm 5.
- 5. i = i + 1
- 6. **end**
- 7. Normalize the digital baseband precoder at the transmitter end as shown in (4.34).

To avoid the increase in each iteration, the objective function (3.17) is minimized at Step 3 and Step 4, and it is known that the objective functions are non-negative. Therefore, the proposed algorithm is guaranteed to converge in a critical point to solve the hybrid precoding problem [10]. The complexity of the proposed algorithm is analyzed in the next subsection and the simulation results in Chapter 6 demonstrate that the proposed algorithm achieves nearly optimal performance with a less computational cost compared with the CG-based algorithm given in [10].

4.4.4 Complexity Analysis

In this section, the complexity of the proposed algorithm is analyzed and compared with the other alternating minimization algorithms. The number of operations required to compute the hybrid precoders (or decoders) for the proposed alternating minimization algorithm based on Riemannian BB and the competing methods are illustrated in Table 4.1. For a given number of transmitter (or receiver) antennas, RF chains, and transmitted symbols, Table 4.1 displays the computational cost of the proposed algorithm and competing methods. Since the complexity provided by the number of additions and subtractions has minor effects, the computations are focused on the number of multiplications and divisions (no. of mult. & div.). As it can be observed, Broyden-Fletcher-Goldfarb-Shanno (BFGS) method [86], [98] has the highest complexity with $O(N_{\rm BS}{}^3N_{\rm RF}{}^3)$ and it cannot be applied for practical use. As previously stated, the OPP algorithm has the lowest computational complexity given by $O(N_{\rm BS}N_{\rm RF}N_{\rm S})$. Although both CG and BB methods have the same complexity $O(N_{\rm BS}N_{\rm RF}N_{\rm S})$, simulation results in Chapter 6 demonstrate that the computational

Table 4.1: Computational Cost of the Proposed and Competing Methods

Number of Multiplications & Divisions $N_{RF} \left(4N_{BS}(N_{RF}N_{s} + N_{s} + 1) + \frac{1}{3}(N_{RF}^{2} + 3N_{RF} - 1) \right)$ BFGS $N_{RF} \left(N_{BS}(2N_{BS}^{2}N_{RF}^{2} + 7N_{BS}N_{RF} + 2N_{RF}N_{s} + 2N_{RF} + 3N_{s} + 3) + \frac{1}{3}(N_{RF}^{2} + 3N_{RF} - 1) \right)$ CG $N_{RF} \left(4N_{BS}(N_{RF}N_{s} + N_{RF} + N_{s} + 4) + \frac{1}{3}(N_{RF}^{2} + 3N_{RF} - 1) \right)$ OPP $N_{RF} \left(2N_{BS}N_{s} + N_{RF}N_{s} + 2N_{RF}^{2} + N_{s}^{2} \right)$

cost of BB is much less than CG. The dominant terms to approximate the time complexities of different algorithms are chosen considering the fact that $N_{\rm BS}\gg N_{\rm RF}$ and $N_{\rm BS}\gg N_{\rm S}$ in the hybrid precoding system.

Chapter 5

PROPOSED ADAPTIVE FUZZY LOGIC-BASED FILTER

In mmWave systems, the noise is generally modeled using the GN model. On the other hand, research findings state that the ambient noise may act non-Gaussian in many physical channels, and the Gaussian mixture model with additive IN as shown in (3.14) is a more realistic approach to express the noise in mmWave channels. Furthermore, although the effects of GN can be reduced by applying the hybrid decoders to the received signal, the IN component should be removed before passing the signal through the decoders. Therefore, in this thesis, a fuzzy logic-based filter is proposed to mitigate the effects of IN and the filter design is introduced in this chapter.

5.1 Receiver Model for Impulsive Noise Environment

The receiver model for the IN environment is shown before in Figure 3.2, where the proposed adaptive fuzzy median filter is added to the hybrid decoder to minimize the effects of the outlier amplitudes. The outlier amplitudes can be considered as the IN and it is aimed to minimize the effects of IN by ordering the samples based on the fuzzy rank. The filter alone is working very well for the IN environment. However, it is observed that the filter is suppressing the information while reducing the effects of the noise for the GN environment. Thus, a novel threshold mechanism is adapted to the design to detect the received packages with IN. A modified Z-score as suggested in [99] is applied to the received signal to detect the outlier amplitudes and it is

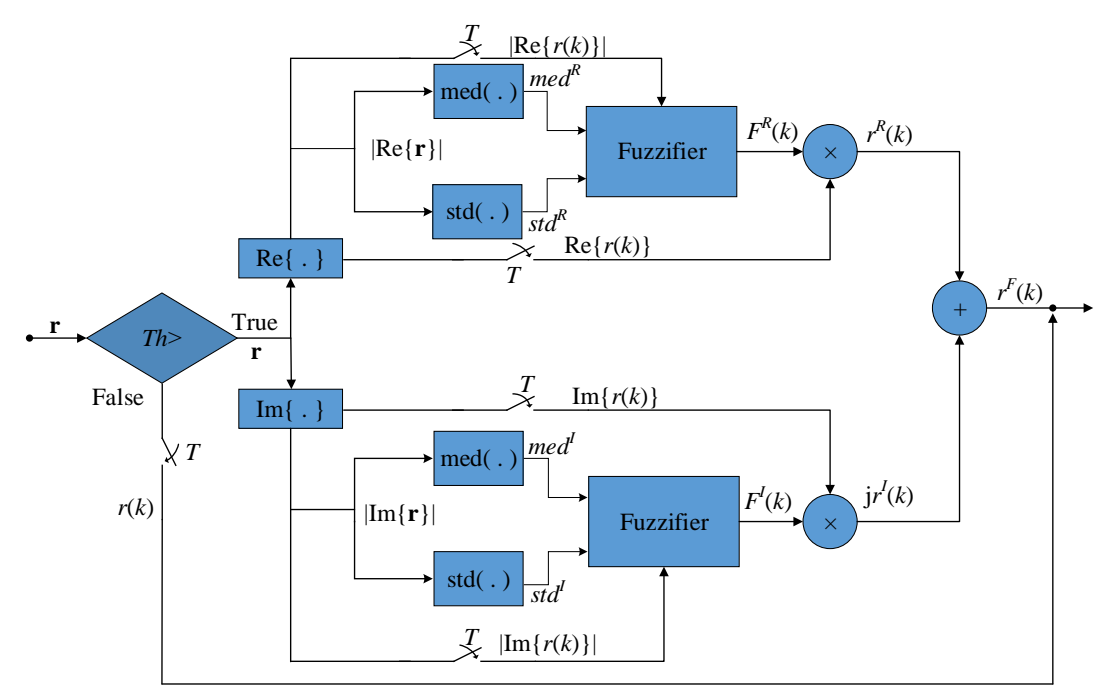


Figure 5.1: Block diagram of the fuzzy median filter at the receiver.

observed that the proposed decoder with the filter that selects a proper threshold is suitable for GN and IN environments. The proposed fuzzy median filter design with the threshold mechanism is explained in the next subsection.

5.1.1 Fuzzy Median Filter Design

The fuzzy median filter is added in front of the receiver and the received signal $\mathbf{r} = [r(1), r(2), ..., r(N_{MS})]$ denoted in (3.4) is passed through the filter to reduce the effects of the IN. It should be noted that the noise term of the \mathbf{r} is represented as the Gaussian mixture model as shown in (3.14). Thus, the block diagram of the proposed fuzzy median filter with the threshold mechanism is shown in Figure 5.1 and the effects of the outlier amplitudes are minimized, which will lead to suppressing IN components.

The filtering process starts with the threshold mechanism to detect the received packages with IN and the details about the threshold mechanism will be explained in

the following subsection. The outlier amplitudes will be detected by the threshold and the signals with the IN components will pass through the fuzzy median filter. Firstly, the received signal is divided into real and imaginary parts, and then the statistical measures of both parts of the received signal are computed as

$$med^{R} = med(|Re\{r\}|), med^{I} = med(|Im\{r\}|)$$
 (5.1)

$$std^{R} = std(|\operatorname{Re}\{\mathbf{r}\}|), std^{I} = std(|\operatorname{Im}\{\mathbf{r}\}|),$$
 (5.2)

where the median of the real and imaginary parts of the \mathbf{r} is denoted as med^R and med^I , respectively, and the standard deviation of the real and imaginary parts of the \mathbf{r} is represented as std^R and std^I , respectively. The real and imaginary parts of the r(k) and the statistic components are then used in the fuzzifier to calculate the Gaussian membership degrees. Thus, the fuzzifier for real and imaginary parts can be derived separately as

$$F^{R}(k) = \exp\left(\frac{-\left||\operatorname{Re}\{r(k)\}| - med^{R}\right|^{2}}{2std^{R}}\right)$$
 (5.3)

$$F^{I}(k) = \exp\left(\frac{-\left||\operatorname{Im}\{r(k)\}| - med^{I}\right|^{2}}{2std^{I}}\right), \tag{5.4}$$

where $F^R(k)$ and $F^I(k)$ denote the real and imaginary parts of the fuzzifier which give the membership degrees of the received signals r(k) by checking their distances with the median. The fuzzifiers are distributed between 0 and 1 based on the membership degrees of r(k) and then they are applied to the received signal elementwise to order each received signal based on the fuzzy rank. Hence, the elements of the received vectors after applying the fuzzy filter can be shown as

$$r^{R}(k) = \operatorname{Re}\{r(k)\} \circ F^{R}(k) \tag{5.5}$$

$$r^{I}(k) = \operatorname{Im}\{r(k)\} \circ F^{I}(k),$$
 (5.6)

where $r^R(k)$ and $r^I(k)$ represent the elements of the real and imaginary parts of the fuzzy median filter output, respectively [54]–[56], [100]. Finally, $r^R(k)$ and $r^I(k)$ are combined in the last stage as

$$r^{F}(k) = r^{R}(k) + jr^{I}(k),$$
 (5.7)

where $r^F(k)$ denotes the output of the fuzzy median filter that can be shown in the vector form as

$$\mathbf{r}^F = [r^F(1), r^F(2), \dots, r^F(N_{MS})]. \tag{5.8}$$

After passing the received signal vector through the fuzzy median filter, the output of the filter is fed into the hybrid decoders, \mathbf{W}_{RF} and \mathbf{W}_{BB} , to obtain the vector \mathbf{y} as shown in (3.6).

5.1.2 Threshold Mechanism to Detect Outlier Amplitudes

A threshold mechanism is designed to detect the outlier amplitudes considered as the IN, and the fuzzy filter is only applied to the received signals with IN samples. The optimal threshold value is selected to enable the proposed filter to perform adaptively in both GN and IN environments. Thus, the Z-score method and the modified Z-score are tested to detect outlier amplitudes in mmWave systems. It is observed that the performance of the simple Z score is poor and the modified Z score can detect the outlier amplitudes with very high precision. In this section, both methods are introduced and the proposed threshold mechanism based on the modified Z-score is given.

5.1.2.1 Z-Score Method to detect Outlier Amplitudes

The Z-Score method is a well-known and commonly used method to detect outlier amplitudes. In this method, the fundamental property of the normal distribution is used, such that if the distribution of \mathbf{r} is $N(\mu, \sigma^2)$, then the vector $\mathbf{z} = (r - \mu)/\sigma$ can

be distributed as N(0,1). Thus, the Z-score for each received signal r(k) can be expressed as

$$Z(k) = \frac{(r(k) - \text{mean}(\mathbf{r}))}{s}$$
 (5.9)

where the denominator coefficient s can be considered as the standard deviation of \mathbf{r} that is denoted as

$$s = \sqrt{\frac{\sum_{k=1}^{N_{MS}} (r(k) - \text{mean}(\mathbf{r}))^2}{N_{MS} - 1}}.$$
 (5.10)

The amplitudes will be labeled as outliers if the absolute value of Z(k) is greater than 3 [99]. Although this method is very simple to implement, the performance is poor in detecting the outliers for small data sets. Besides, this method only uses the mean and standard deviation as estimators, which can be affected by a few outliers (even one outlier). Therefore, alternative Z-score methods are developed to ensure resistant estimators, and the modified Z-score with better estimators is proposed to identify outlier amplitudes [99].

5.1.2.2 Modified Z-Score to Detect Outlier Amplitudes

To detect the outliers with high precision, the estimators should be selected carefully and they need to be stable for minor changes in the samples. This kind of estimator has a high breakdown point. The breakdown point of an estimator is the largest set of samples that can be substituted with the random values by not causing an infinite estimated value. Since the mean and standard deviation have high breakdown points, they are replaced with the median and Median Absolute Deviation (MAD), respectively [99]. Thus, the modified Z-score to detect IN samples is given by

$$M(k) = \frac{0.6745(r(k) - med(\mathbf{r}))}{MAD},$$
(5.11)

where MAD can be calculated as

MAD =
$$\frac{1}{N_{\text{MS}}} \sum_{k=1}^{N_{\text{MS}}} |r(k) - med(\mathbf{r})|.$$
 (5.12)

In this method, the constant 0.6745 is used in (5.11) since $\mathbb{E}[MAD] = 0.6745\sigma$, and the potential outlier amplitudes can be detected when the absolute value of M(k) is higher than 3.5 [99].

This method is still not too complex and performs very accurately to label the outlier amplitudes. Based on the study in [99], the optimal threshold is selected as 3.5 and the samples are considered as IN for |M(k)| > 3.5. Simulation results demonstrate that the optimal threshold is selected properly, and the proposed fuzzy median filter with threshold mechanism mitigates the IN better than the competing methods in both IN and GN environments.

Chapter 6

SIMULATION RESULTS

In this chapter, the performance of the proposed Riemannian BB-based algorithm is evaluated with different aspects and compared with the existing algorithms. Besides, numerical simulation results of the proposed decoder with the fuzzy median filter are demonstrated for different scenarios in IN environment.

Throughout the simulations, channel parameters in (3.8) are selected as $N_{\rm cl}=5$ clusters, and $N_{\rm ray}=10$ rays and it is assumed that the perfect channel information is known. The arrival and departure angles are distributed randomly which follows the uniform distribution in $[0, 2\pi]$ and the angular spread is set as 10. Furthermore, each cluster is organized to have unit average power as $\sigma_{\alpha,i}^2=1$, and the SNR in the receiver side is defined as SNR = ρ/σ_n^2 . The system is assumed to operate at 28 GHz carrier frequency with a bandwidth of 100 MHz, and all the simulation results are executed in MATLAB 2018b while each simulation point is averaged over 1000 independent realizations. The antenna elements are placed with a half wavelength distance and the number of BS antennas and MS antennas is assumed to be $N_{\rm BS}=144$ and $N_{\rm MS}=36$, respectively. Besides, the phases of the analog precoder ${\bf F}_{\rm RF}$ is initialized to follow a uniform distribution in $[0,2\pi]$ for the alternating minimization algorithms.

6.1 Simulation Results for GN Environment

In this section, simulations are performed to find out the spectral efficiency, BER, coverage probability, and no. of mult. & div. of the proposed Riemannain BB method under GN defined in (3.5) together with the competing methods.

Firstly, the spectral efficiency performance is evaluated using (3.15) for various SNR values, where the number of transmitted symbols and RF chains are chosen as N_s = $N_{\rm RF}=3$. Based on that assumption, Figure 6.1 illustrates the spectral efficiency versus SNR under GN for the proposed Riemannian BB method and the competing methods. It can be seen that the spectral efficiency performances of the CG, BFGS, OPP, GP [101], and the proposed BB algorithms are almost identical. On the other hand, the Penalty Function (PF) and Sequential Quadratic Programming (SQP) [86] algorithms have poorer performance, and there is a gap between the rest of the algorithms. It should be also noted that the Optimal Precoder (OP) is serving as a benchmark that represents the performance of the fully digital precoding, and all the algorithms except PF and SQP are performing very close to the optimal scenario. In addition, Figure 6.2 demonstrates the spectral efficiency performance of the proposed and competing methods with respect to the different number of RF chains. In this figure, the number of transmitted symbols and SNR value are set to be $N_s = 6$ and SNR = 0, respectively. The GP algorithm is not included since the authors in [101] simulate their results for the settings presented in Figure 6.1. Here, although the CG, BFGS, OPP, and the proposed BB method have a very close spectral efficiency performance for the equal case scenario of the number of transmitted symbols and RF chains, $N_{\rm s}=N_{\rm RF},$ the performance of the OPP algorithm is not improving like the other algorithms while

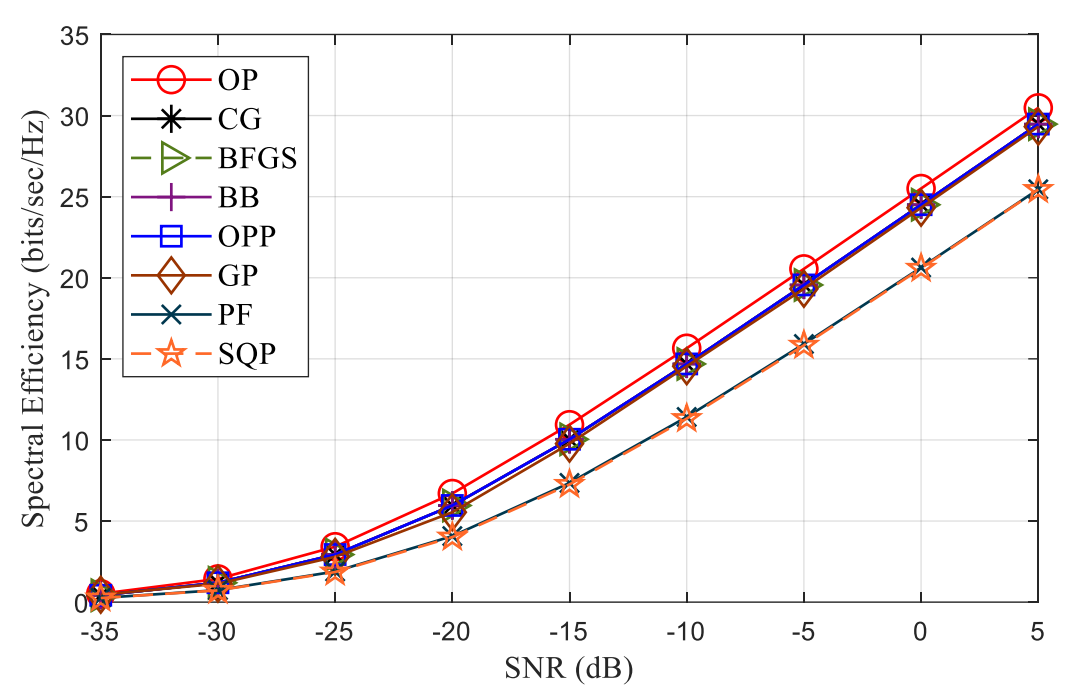


Figure 6.1: Spectral Efficiency versus SNR under GN.

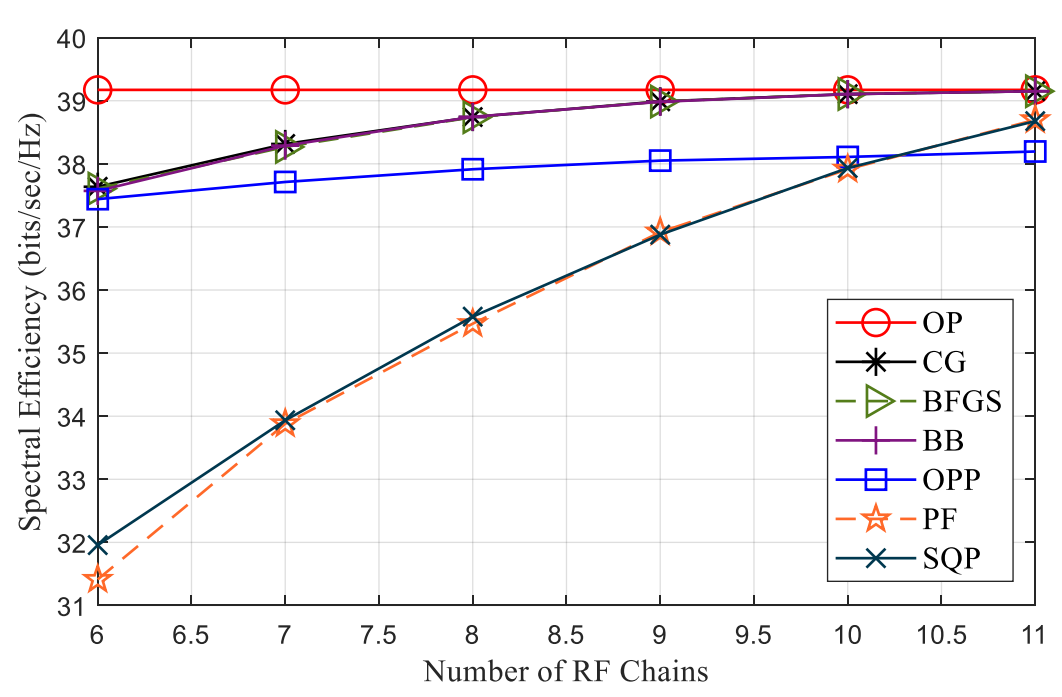


Figure 6.2: Spectral Efficiency versus the number of RF chains under GN.

increasing the number of RF chains. It is observed that the performance of the CG, BFGS, and the proposed BB algorithm is approaching the performance of the OP when the difference between the $N_{\rm RF}$ and $N_{\rm S}$ is increased, and based on this result, we can

claim that the performances of these algorithms are same as the OP for $N_{\rm RF} \geq 2N_{\rm s}$. Moreover, PF and SQP algorithms still have poor performances, and it is shown that these algorithms perform better than the OPP algorithm for $N_{\rm RF} > 10$.

Since BFGS is too complex for practical implementation and PF and SQP methods performing very poorly compared to the other algorithms, these algorithms are not included in the rest of the figures. To have a better understanding of the performances of the competing methods, additional performance parameters such as BER, coverage probability, and no. of mult. & div. are evaluated. In this regard, Figure 6.3 plots the coverage probability defined as $\mathcal{P}(R > Th)$ for SNR = 0, $N_{\rm S}$ = 4, and $N_{\rm RF}$ = 5, where R denotes the achievable rate and Th represents the arbitrary threshold value. It can be seen that the coverage probability of the proposed BB method is almost identical with the CG with a close performance to OP, while OPP achieves slightly poorer performance. Besides, Figure 6.4 shows the BER performance of the BB method with the competing methods for various SNR values. The same setup is used as the Figure 6.3 and it is observed that the CG method is performing better than the other alternating minimization methods with the lowest BER. Additionally, the proposed BB method has a close performance to CG and achieves nearly optimal performance.

Figure 6.5 depicts the spectral efficiency performance for different numbers of transmitter and receiver antennas. In Figure 6.5 (a), the number of MS antennas is fixed to be 36, and the same setup is used as Figure 6.3 and Figure 6.4. It is shown that the spectral efficiency performance of all the algorithms is improving, while the transmitter antennas are increasing. Furthermore, Figure 6.5 (b) has the same setup except for the number of BS antennas which is fixed to be 144, and it is observed that

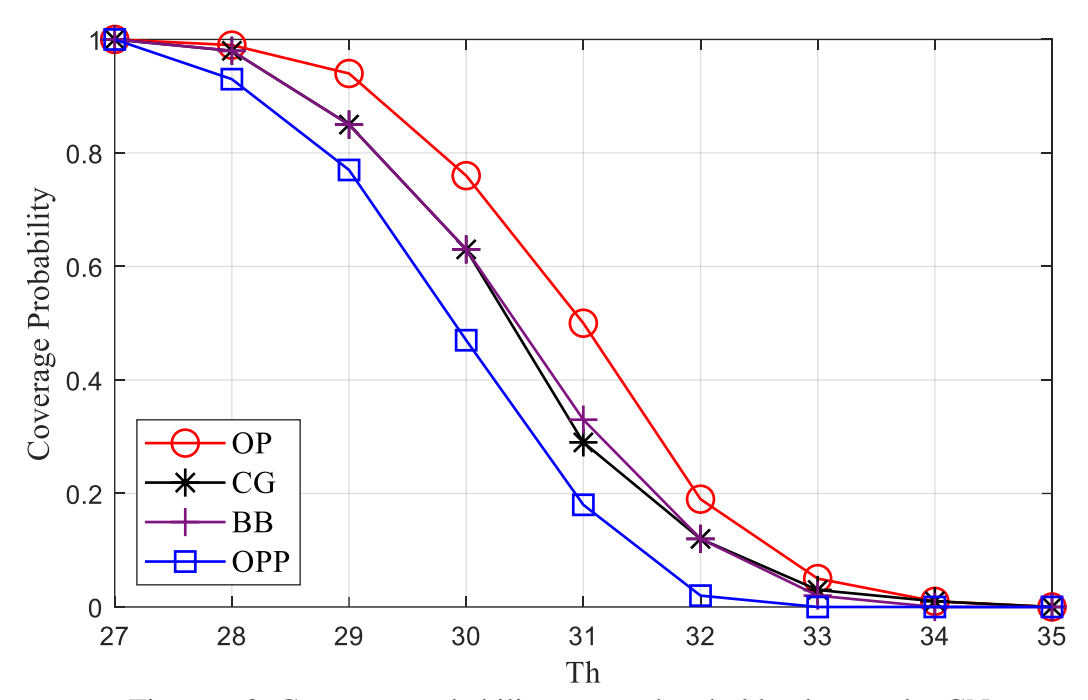


Figure 6.3: Coverage probability versus threshold values under GN.

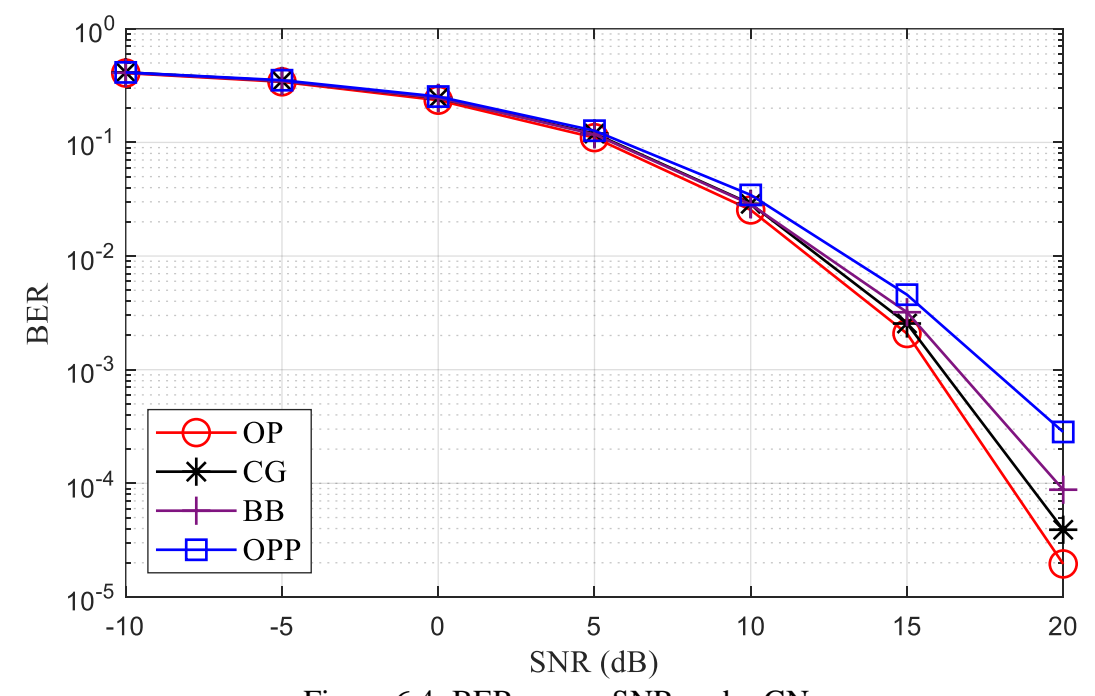


Figure 6.4: BER versus SNR under GN.

the spectral efficiency is also increasing for the higher number of receiver antennas. Both figures show that the BB and CG methods have equivalent performance, but OPP has a lower performance. Based on the outcomes from Figure 6.5, it can be said that the implementation of massive MIMO systems can improve spectral efficiency performance, and increasing the antennas has a direct effect on the performance. Also, it can be seen that the OPP algorithm only achieves a close performance to the other algorithms and the OP for the equal number of transmitted symbols and RF chains. Therefore, the OPP method has an unrealistic restriction for the real-time practical implementation, and we focus on the CG and BB algorithms to find the optimal solution for hybrid precoding problem in terms of complexity.

Figure 6.6 displays the no. of mult. & div. required for the proposed BB algorithm and the competing CG method for several $N_{\rm BS}$, and $N_{\rm RF}$ in which the numerical results are calculated with the help of Table 4.1. Both methods are simulated considering that the number of MS antennas are assumed to be $N_{\rm MS}=36$, and the number of transmitted symbols is selected as $N_s = 4$. In this regard, Figure 6.6 (a) plots the no. of mult. & div. versus the $N_{\rm BS}$ for $N_{\rm RF}=5$, and Figure 6.6 (b) plots no. of mult. & div. versus the $N_{\rm RF}$ for $N_{\rm BS}=144$. It is remarked that to provide the almost same performance with CG, the proposed BB method requires less computational cost. Besides, the computational gap between the two algorithms is increasing for the higher number of $N_{\rm BS}$ and $N_{\rm RF}$. For a better understanding of the dramatic difference between the two algorithms, the improvement of the no. of. mult. & div. of the proposed BB algorithm over the CG under several scenarios, and the numerical representation of the no. of. mult. & div. for both algorithms are illustrated in Table 6.1 and Table 6.2, respectively. It is indicated that the improvement in the computational cost is constant for the different number of BS antennas, while it is slightly decreasing for the higher number of RF chains.

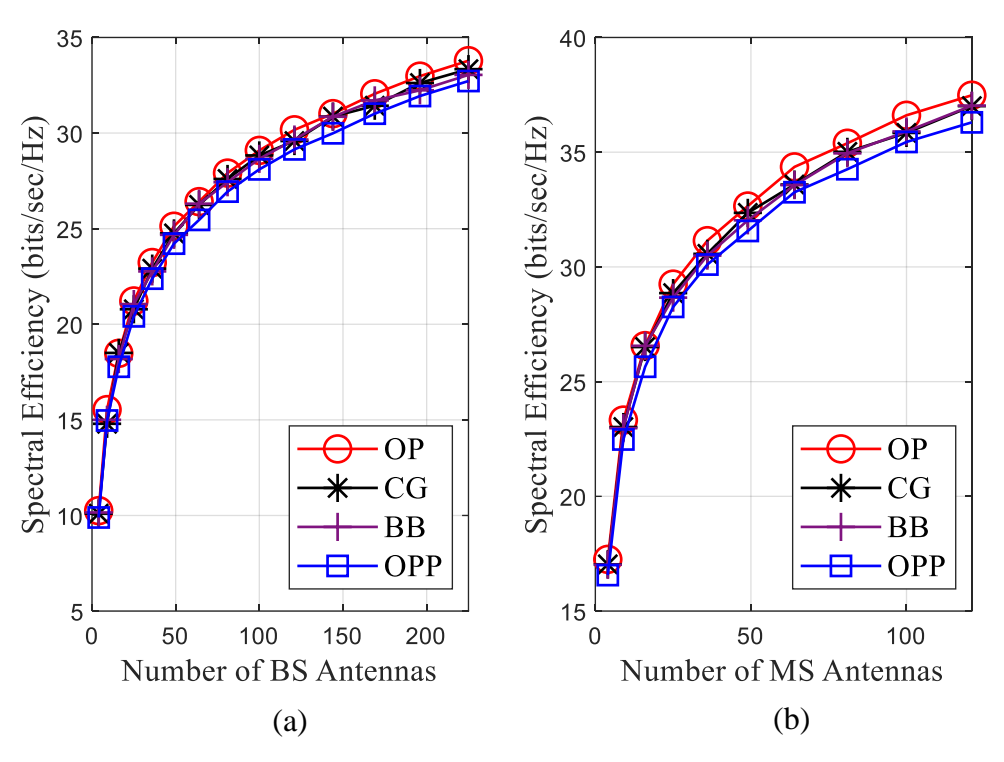


Figure 6.5: (a) Spectral efficiency versus the number of BS antennas for $N_{\rm MS}=36$, and (b) the number of MS antennas for $N_{\rm BS}=144$ under GN.

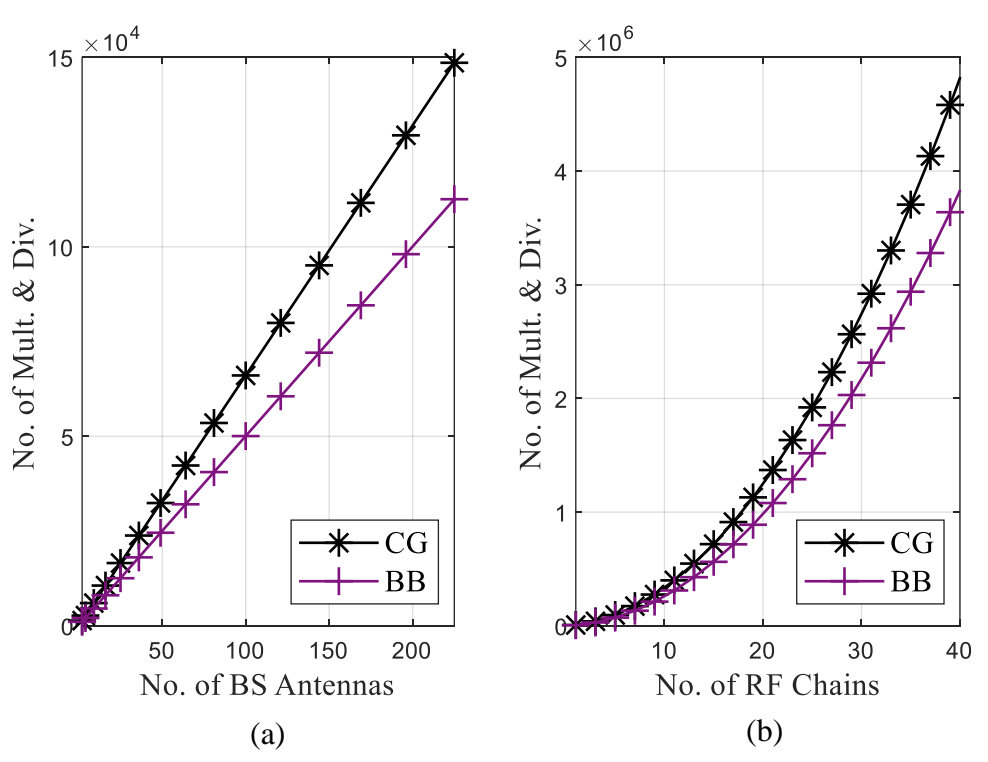


Figure 6.6: (a) The number of mult. & div. versus the number of BS antennas, and (b) the number of mult. & div. versus the number of RF chains.

Table 6.1: Improvement of Computational Cost of BB over CG

N_{RF}	N_{BS}	Improvement (%)*	$N_{\rm BS}$	N_{RF}	Improvement (%)*
5	121	24.22	144	4	24.98
	144	24.22		6	23.66
	169	24.22		8	22.89

Table 6.2: Numerical Representation of the Computational Costs

$N_{\rm RF}=5, N_{\rm BS}=144$	BB	BFGS	CG	OPP
No. of Mult. & Div.	7.207×10^4	7.502×10^{8}	9.511×10^4	6.190×10^3

^{*} Improvement = $\frac{\text{no. of mult. \& div.(CG)} - \text{no. of mult. \& div.(BB)}}{\text{no. of mult. \& div.(CG)}} \times 100.$

6.2 Simulation Results for IN Environment

In this section, the numerical simulation results of the proposed decoder with the fuzzy median filter to mitigate IN under different scenarios are demonstrated, and the results are compared with the methods proposed in [50]. BER and the spectral efficiency performances of the system are calculated under the IN using the Gaussian mixture noise model expressed in (3.14), where the proposed BB algorithm is applied to solve the hybrid precoders and decoders. It is assumed that the $N_{\rm s}=1$ symbol with 256 packets are transmitted through $N_{\rm RF}=6$ RF chains, and the transmitted signal is modulated using 16-QAM, besides, the SINR is set to be -10 dB.

Figure 6.7 shows the BER performance of the system with a fuzzy median filter for different SNR values in the Gaussian channel ($\epsilon = 0$). It is observed that the

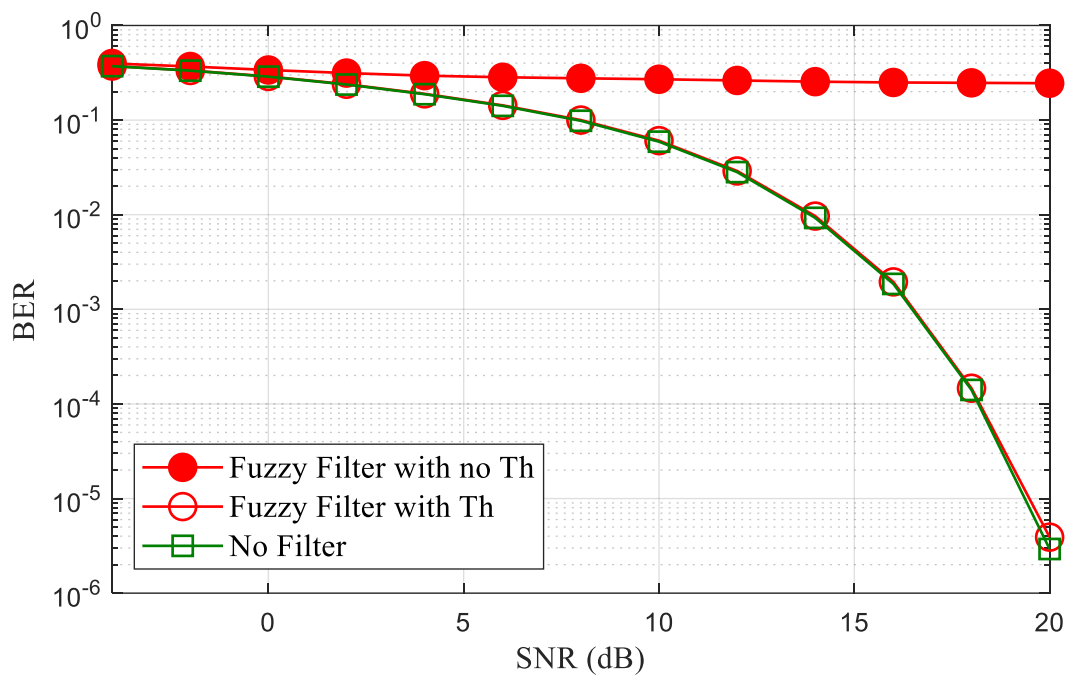


Figure 6.7: BER versus SNR in Gaussian channel ($\epsilon = 0$) for fuzzy filter with threshold and without threshold.

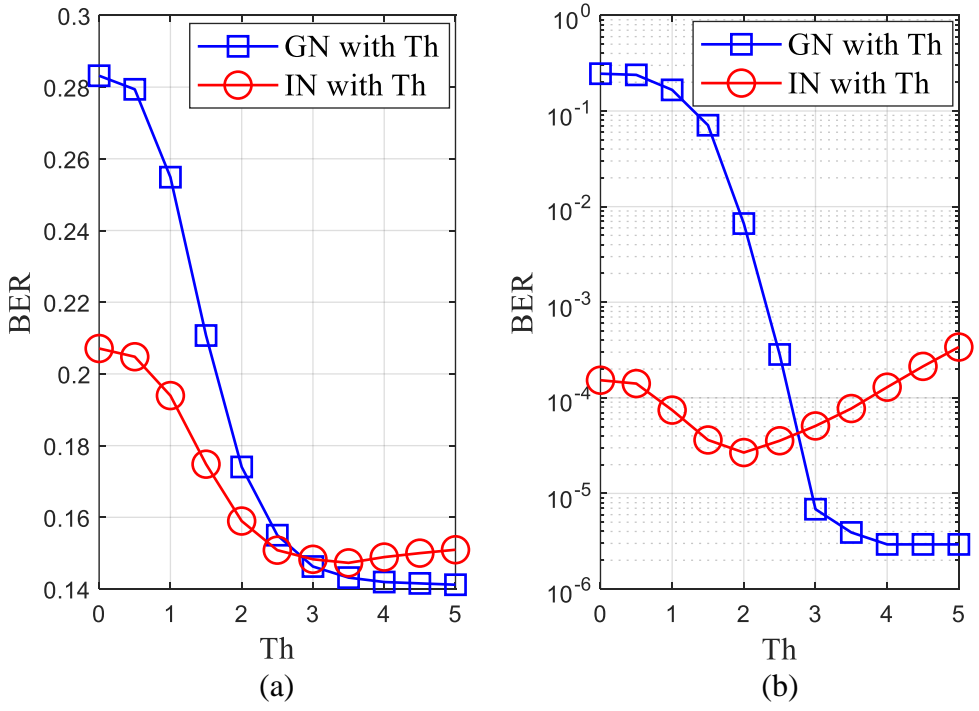


Figure 6.8: BER versus noise threshold in Gaussian channel ($\epsilon = 0$) and IN channel ($\epsilon = 0.02$) (a) SNR = 6 dB (b) SNR = 20 dB.

performance of the system is very poor when there is no threshold used in the filter and the system without the fuzzy filter is served as a benchmark. Thus, a threshold mechanism is developed as suggested in Chapter 5 and applied together with the fuzzy median filter to identify the IN samples. In Figure 6.8, the BER performance of the system with fuzzy median filter is tested for different threshold values at 6 dB and 20 dB SNR values to select the optimal threshold. To achieve a maximum gain in GN and minimum loss in IN with $\epsilon = 0.02$, the threshold can be chosen between 2 and 4. Therefore, we have decided to choose the optimal threshold as 3.5 considering the theoretical proofs given in [99]. After threshold implementation, the fuzzy median filter performs almost the same as the benchmark as illustrated in Figure 6.7.

Figure 6.9 demonstrates the SNR versus BER of the system with different IN mitigation filters in IN channel for $\epsilon=0.02$ and $\epsilon=0.04$. It is indicated that the fuzzy median filter with an optimal threshold performs much better than the blanking and clipping filters for both IN channels. Besides, the clipping filter achieves the worst performance among the competing methods, and the system without any IN filter has a very deficient performance. Furthermore, the BER performance of the competing filters in IN channel for various epsilon (ϵ) values are investigated. In this regard, BER versus epsilon at SNR values 5 dB, 10 dB, and 20 dB are presented in Figure 6.10. The results show that the proposed fuzzy median filter has the best performance for each epsilon and SNR value while the gap with the competing methods is increasing for low epsilon values at 20 dB.

The main aim of this thesis is to maximize the spectral efficiency of the mmWave hybrid massive MIMO system. Hence, the spectral efficiency of the proposed fuzzy

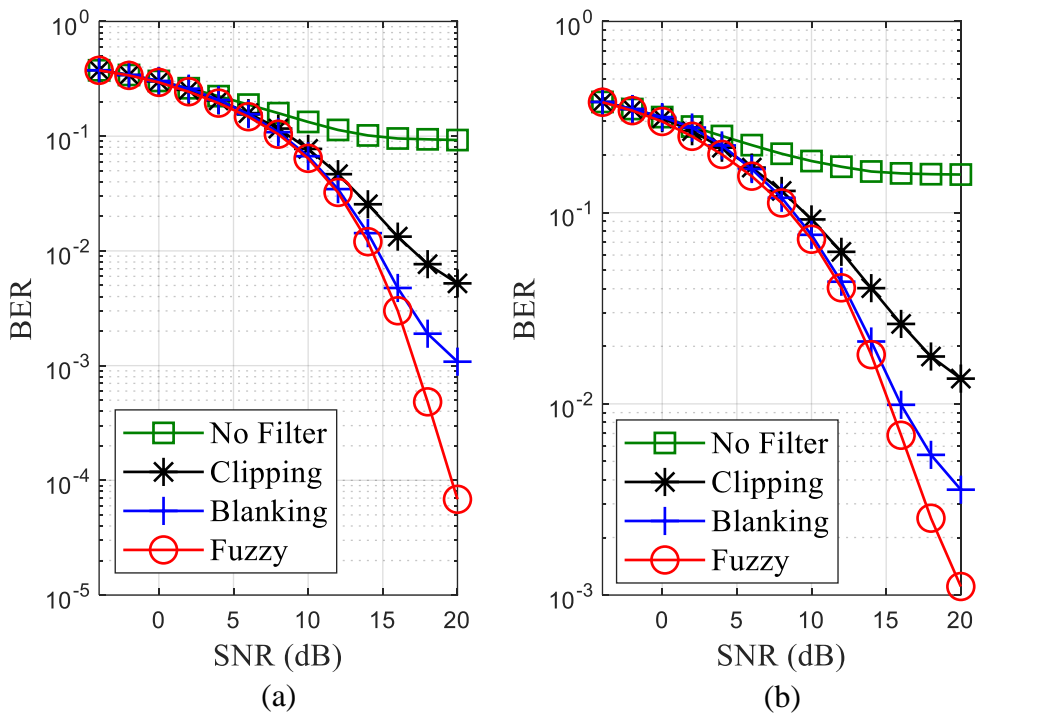


Figure 6.9: BER versus SNR in IN channel (a) ($\epsilon = 0.02$), and (b) ($\epsilon = 0.04$)

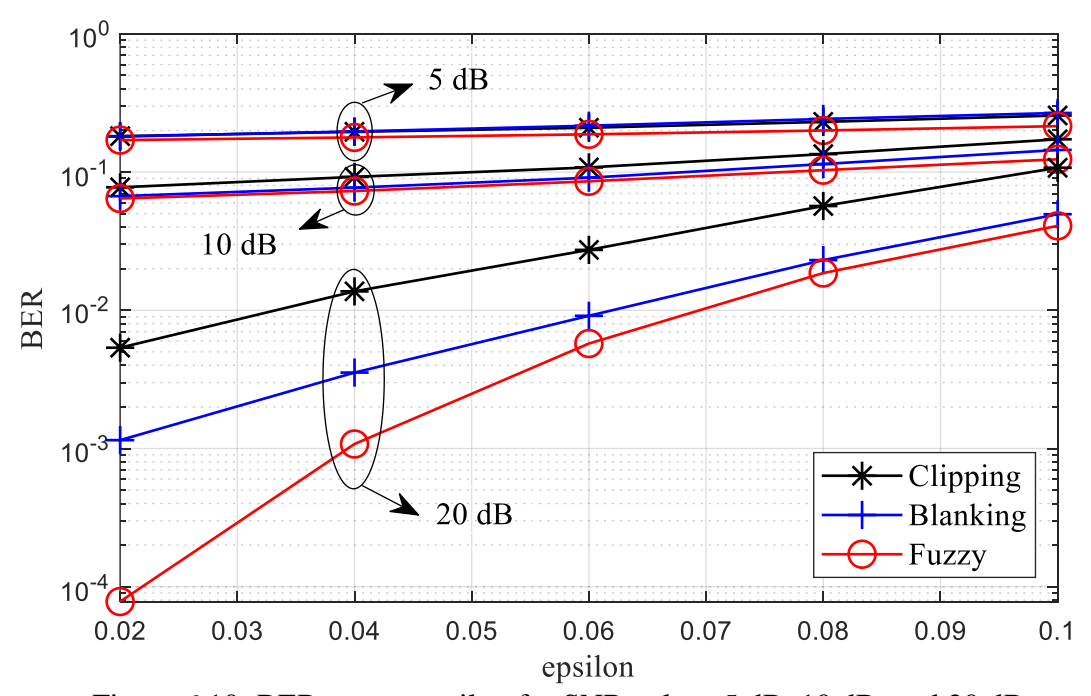


Figure 6.10: BER versus epsilon for SNR values 5 dB, 10 dB, and 20 dB

median filter with hybrid precoding based on the Riemannian BB algorithm is evaluated using (3.15) and compared with the competing IN filters. Figure 6.11 plots

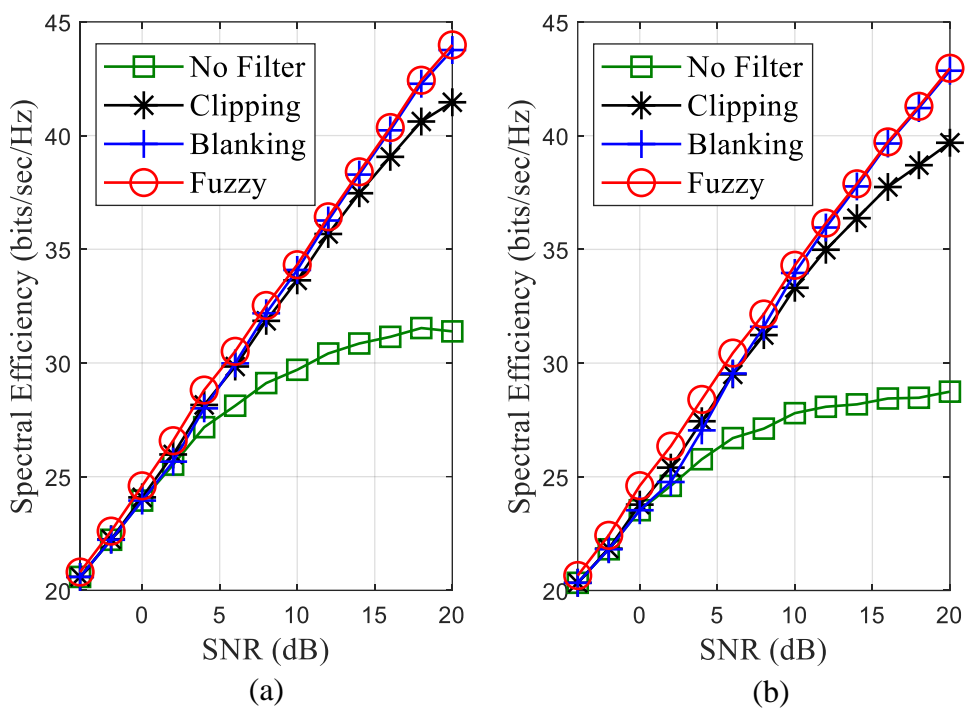


Figure 6.11: Spectral efficiency versus SNR in IN channel (a) ($\epsilon = 0.02$), and ($\epsilon = 0.04$)

the spectral efficiency performance of the system with fuzzy median filter in the receiver for various SNR values under IN, where $\epsilon=0.02$ and $\epsilon=0.04$, and the simulation results are compared with the competing algorithms. It is shown that the spectral efficiency results are parallel to the previous BER results in which the proposed fuzzy median filter achieves a better performance than the competing methods, and the performance is improved enormously compared with the system without any IN filter implementation.

The simulation results clearly show that the fuzzy median filter with the optimal threshold successfully reduces the IN effects and achieves a better BER and spectral efficiency than the existing algorithms. It is also observed that the IN samples distort the received signal extremely and should be suppressed before passing through the hybrid decoders with the help of IN filters. Additionally, outlier amplitudes are

detected using the optimal threshold and this allows the system to work in both GN and IN environments.

Chapter 7

CONCLUSIONS AND FUTURE WORK

7.1 Conclusions

This thesis mainly focuses on maximizing the spectral efficiency of the mmWave hybrid massive MIMO systems using alternating minimization techniques. The alternating minimization method is made up of two stages, where the digital baseband precoder is obtained in the first stage using a least-square solution, and in the second stage, the Riemannian BB method is proposed to solve the analog RF precoder problem. Additionally, the Gaussian mixture model with additive IN is employed to express the noise in mmWave systems and a fuzzy median filter is designed to mitigate the IN.

In this thesis, a new approach is built for hybrid precoding design in mmWave MIMO systems under GN and it is aimed to achieve nearly optimal performance with less computational cost than the competing methods. In this regard, the two-staged alternating minimization algorithm based on the Riemannian BB method is proposed. Simulations are performed to calculate the spectral efficiency, BER, and the coverage probability of the proposed method together with the existing methods in the literature. It is shown that the proposed method requires less computational cost than the well-known CG algorithm to achieve almost the same performance. Besides, in spite of higher complexity than the OPP method, the proposed method performs much better than the OPP method when the number of transmitted symbols and RF chains are not

equal to each other. The restrictions that occurred in the OPP algorithm is avoided and it is observed that the spectral efficiency performance of the proposed algorithm is approaching the fully digital precoders defined as OP for $N_{\rm RF} \geq 2N_s$. Moreover, the performance of the BB method is much better than the PF and SQP while obtaining an identical performance with CG, BFGS, and GP algorithms. Since the proposed BB method has less complexity than the CG and BFGS, this method can be preferred for practical implementation.

The mmWave hybrid MIMO system is also investigated under a different noise model considering the IN effects. Additive IN is added to the received signal using the Gaussian mixture model and the Riemannian BB algorithm is applied to solve the hybrid precoders and decoders under IN. It is indicated that the IN should be suppressed before passing through the decoders. Therefore, a fuzzy median filter with a novel threshold mechanism is designed to reduce the effects of the IN in mmWave massive MIMO systems. The proposed filter is attached at the receiver before the hybrid decoders to detect the outlier amplitudes considered as the IN. The proposed filter detects the received signals with IN with the help of the threshold mechanism and it is illustrated that the system is working for both GN and IN environments. The optimal threshold is selected by testing the filter for various threshold values and it is observed that the threshold is selected properly considering the theoretical proofs. BER and spectral efficiency of the fuzzy median filter are evaluated and compared with the clipping and blanking filters. The simulation results demonstrate that the fuzzy median filter performs better than the clipping and blanking filters in terms of detection and mitigation of IN samples. In addition, the performance of the system is improved enormously when it is compared with the results without any IN filter.

7.2 Future Work

In the literature, the mmWave MIMO systems are mostly investigated for single-user scenario and there is a need for further investigation in multi-user environment. The multi-user interference effects can be taken into consideration and the alternating minimization methods can be applied to cancel the interference. It will be interesting to adapt the proposed Riemannian BB algorithm to the multi-user and a similar approach as shown in [102] can be used to solve the multi-user hybrid precoding problem with the help of alternating minimization techniques. Besides, convergence analysis of different alternating minimization techniques can be evaluated and the hybrid precoder can be designed considering the channel training and feedback. Finally, more IN mitigation filters can be examined and compared with the proposed fuzzy logic-based filter to improve the performance of the mmWave system under IN.

REFERENCES

- [1] J. Widmer *et al.*, "5G radio access above 6 GHz," *Trans. Emerg. Telecommun. Technol.*, vol. 27, no. 9, pp. 1160–1167, 2016, doi: 10.1002/ett.3076.
- [2] M. H. Alsharif and R. Nordin, "Evolution towards fifth generation (5G) wireless networks: Current trends and challenges in the deployment of millimetre wave, massive MIMO, and small cells," *Telecommun. Syst.*, vol. 64, no. 4, pp. 617–637, 2017, doi: 10.1007/s11235-016-0195-x.
- [3] L. Su, Y. Niu, A. V. Vasilakos, Y. Li, and D. Jin, "A survey of millimeter wave communications (mmWave) for 5G: opportunities and challenges," *Wirel. Networks*, vol. 21, no. 8, pp. 2657–2676, 2015, doi: 10.1007/s11276-015-0942-z.
- [4] T. S. Rappaport *et al.*, "Millimeter Wave Mobile Communications for 5G Cellular: It Will Work!," *IEEE Access*, vol. 1, pp. 335–349, 2013, doi: 10.1109/ACCESS.2013.2260813.
- [5] Z. Pi and F. Khan, "An introduction to millimeter-wave mobile broadband systems," *IEEE Commun. Mag.*, vol. 49, no. 6, pp. 101–107, 2011, doi: 10.1109/MCOM.2011.5783993.
- [6] M. Vu and A. Paulraj, "MIMO wireless linear precoding," *IEEE Signal Process*. *Mag.*, vol. 24, no. 5, pp. 86–105, 2007, doi: 10.1109/MSP.2007.904811.

- [7] A. Alkhateeb, J. Mo, N. González-Prelcic, and R. W. Heath, "MIMO precoding and combining solutions for millimeter-wave systems," *IEEE Commun. Mag.*, 2014, doi: 10.1109/MCOM.2014.6979963.
- [8] O. El Ayach, S. Rajagopal, S. Abu-Surra, Z. Pi, and R. W. Heath, "Spatially sparse precoding in millimeter wave MIMO systems," *IEEE Trans. Wirel. Commun.*, vol. 13, no. 3, pp. 1499–1513, 2014, doi: 10.1109/TWC.2014.011714.130846.
- [9] A. Salh *et al.*, "Low Computational Complexity for Optimizing Energy Efficiency in mm-wave Hybrid Precoding System for 5G," *IEEE Access*, vol. 10, pp. 4714–4727, 2022, doi: 10.1109/ACCESS.2021.3139338.
- [10] X. Yu, J. C. Shen, J. Zhang, and K. B. Letaief, "Alternating Minimization Algorithms for Hybrid Precoding in Millimeter Wave MIMO Systems," *IEEE J. Sel. Top. Signal Process.*, vol. 10, no. 3, pp. 485–500, 2016, doi: 10.1109/JSTSP.2016.2523903.
- [11] C. Rusu, R. Mendez-Rial, N. Gonzalez-Prelcic, and R. W. Heath, "Low Complexity Hybrid Precoding Strategies for Millimeter Wave Communication Systems," *IEEE Trans. Wirel. Commun.*, vol. 15, no. 12, pp. 8380–8393, 2016, doi: 10.1109/TWC.2016.2614495.
- [12] J. Barzilai and J. M. Borwein, "Two-point step size gradient methods," *IMA J. Numer. Anal.*, 1988, doi: 10.1093/imanum/8.1.141.

- [13] Y. H. Dai and L. Z. Liao, "R-linear convergence of the Barzilai and Borwein gradient method," *IMA J. Numer. Anal.*, 2002, doi: 10.1093/imanum/22.1.1.
- [14] B. Iannazzo and M. Porcelli, "The Riemannian Barzilai-Borwein method with nonmonotone line search and the matrix geometric mean computation," *IMA J. Numer. Anal.*, vol. 38, no. 1, pp. 495–517, 2018, doi: 10.1093/imanum/drx015.
- [15] E. Telatar, "Capacity of multi-antenna Gaussian channels," *Eur. Trans. Telecommun.*, 1999, doi: 10.1002/ett.4460100604.
- [16] G. J. Foschini and M. J. Gans, "On Limits of Wireless Communications in a Fading Environment when Using Multiple Antennas," *Wirel. Pers. Commun.*, 1998, doi: 10.1023/A:1008889222784.
- [17] R. W. Heath, N. Gonzalez-Prelcic, S. Rangan, W. Roh, and A. M. Sayeed, "An Overview of Signal Processing Techniques for Millimeter Wave MIMO Systems," *IEEE J. Sel. Top. Signal Process.*, vol. 10, no. 3, pp. 436–453, 2016, doi: 10.1109/JSTSP.2016.2523924.
- [18] Y. Ding, K. J. Kim, T. Koike-Akino, M. Pajovic, P. Wang, and P. Orlik, "Spatial Scattering Modulation for Uplink Millimeter-Wave Systems," *IEEE Commun. Lett.*, vol. 21, no. 7, pp. 1493–1496, Jul. 2017, doi: 10.1109/LCOMM.2017.2684126.
- [19] R. Mesleh and A. Younis, "Capacity analysis for LOS millimeter–wave quadrature spatial modulation," *Wirel. Networks*, vol. 24, no. 6, pp. 1905–1914,

- Aug. 2018, doi: 10.1007/s11276-017-1444-y.
- [20] X. Lin, T. Tian, C. Zhao, and B. Li, "On the Spatial Modulation for 60 GHz Millimeter Wave Communications with Nonlinear Distortions," in *Proceedings* of the 2015 International Conference on Communications, Signal Processing, and Systems, 2016, pp. 471–478.
- [21] A. Kafizov, A. Elzanaty, and M.-S. Alouini, "Probabilistic Shaping Based Spatial Modulation for Spectral-Efficient VLC," *IEEE Trans. Wirel. Commun.*, vol. 1276, no. c, pp. 1–1, 2022, doi: 10.1109/TWC.2022.3164991.
- [22] S. A. Busari, K. M. S. Huq, S. Mumtaz, L. Dai, and J. Rodriguez, "Millimeter-Wave Massive MIMO Communication for Future Wireless Systems: A Survey," *IEEE Commun. Surv. Tutorials*, vol. 20, no. 2, pp. 836–869, 2018, doi: 10.1109/COMST.2017.2787460.
- [23] T. Kebede, Y. Wondie, J. Steinbrunn, H. B. Kassa, and K. T. Kornegay, "Precoding and Beamforming Techniques in mmWave-Massive MIMO: Performance Assessment," *IEEE Access*, vol. 10, pp. 16365–16387, 2022, doi: 10.1109/ACCESS.2022.3149301.
- [24] X. Gao, L. Dai, Z. Gao, T. Xie, and Z. Wang, "Precoding for mmWave massive MIMO," in *mmWave Massive MIMO: A Paradigm for 5G*, 2017.
- [25] D. Gesbert, M. Shafi, D. S. Shiu, P. J. Smith, and A. Naguib, "From theory to practice: An overview of MIMO space-time coded wireless systems," *IEEE J.*

- Sel. Areas Commun., 2003, doi: 10.1109/JSAC.2003.809458.
- [26] X. Gao, L. Dai, S. Han, I. Chih-Lin, and R. W. Heath, "Energy-Efficient Hybrid Analog and Digital Precoding for MmWave MIMO Systems with Large Antenna Arrays," *IEEE J. Sel. Areas Commun.*, 2016, doi: 10.1109/JSAC.2016.2549418.
- [27] Y. Y. Lee, C. H. Wang, and Y. H. Huang, "A Hybrid RF/baseband precoding processor based on parallel-index-selection matrix-inversion-bypass simultaneous orthogonal matching pursuit for millimeter wave MIMO systems," *IEEE Trans. Signal Process.*, 2015, doi: 10.1109/TSP.2014.2370947.
- [28] J. Lee and Y. H. Lee, "AF relaying for millimeter wave communication systems with hybrid RF/baseband MIMO processing," in 2014 IEEE International Conference on Communications, ICC 2014, 2014, pp. 5838–5842, doi: 10.1109/ICC.2014.6884253.
- [29] M. Mulla, A. H. Ulusoy, A. Rizaner, and H. Amca, "Barzilai-Borwein Gradient Algorithm Based Alternating Minimization for Single User Millimeter Wave Systems," *IEEE Wirel. Commun. Lett.*, 2020, doi: 10.1109/LWC.2019.2960691.
- [30] R. Everson, "Orthogonal, but not Orthonormal, Procrustes Problems," *Convergence*, no. 4, pp. 1–11, 1997.
- [31] J. C. Gower and G. B. Dijksterhuis, *Procrustes Problems*. Oxford University

Press, 2007.

- [32] P.-A. Absil, R. Mahony, and R. Sepulchre, *Optimization Algorithms on Matrix Manifolds*. Princeton University Press, 2008.
- [33] J. M. Lee, *Introduction to Smooth Manifolds*. Springer Science & Business Media, 2012.
- [34] B. Q. Vuong, H. T. Huynh, and H. N. Do, "Monte-Carlo performance analysis of OFDM system in the presence of multi-path fading environment and non-Gaussian noise," in *Proceedings 2018 2nd International Conference on Recent Advances in Signal Processing, Telecommunications and Computing, SIGTELCOM 2018*, Mar. 2018, vol. 2018-Janua, pp. 230–235, doi: 10.1109/SIGTELCOM.2018.8325796.
- [35] D. Middleton, *An introduction to: Statistical communication theory*. Wiley-IEEE Press, 2009.
- [36] X. Wang and H. V. Poor, "Robust multiuser detection in non-gaussian channels," *IEEE Trans. Signal Process.*, 1999, doi: 10.1109/78.740103.
- [37] F. Rouissi, A. J. H. Vinck, and A. Ghazel, "On the simulation of the Middleton Class-A noise model for single- and multi-carrier modulation in power line communication," *Telecommun. Syst.*, no. 0123456789, 2021, doi: 10.1007/s11235-020-00746-x.

- [38] M. S. Alam, B. Selim, and G. Kaddoum, "Analysis and Comparison of Several Mitigation Techniques for Middleton Class-A Noise," in 2019 IEEE Latin-American Conference on Communications (LATINCOM), Nov. 2019, pp. 1–6, doi: 10.1109/LATINCOM48065.2019.8938020.
- [39] K. Hagglund and E. Axell, "Adaptive Demodulation in Class a Impulse Noise Channels," in 2019 IEEE Global Communications Conference (GLOBECOM),

 Dec. 2019, pp. 1–6, doi: 10.1109/GLOBECOM38437.2019.9013968.
- [40] S. Moaveninejad, A. Kumar, M. Elgenedy, M. Magarini, N. Al-Dhahir, and A. M. Tonello, "Gaussian-Middleton Classification of Cyclostationary Correlated Noise in Hybrid MIMO-OFDM WiNPLC," in 2019 IEEE International Conference on Communications (ICC), May 2019, pp. 1–7, doi: 10.1109/ICC.2019.8761152.
- [41] L. Liu and M. G. Amin, "Performance analysis of GPS receivers in non-Gaussian noise incorporating precorrelation filter and sampling rate," *IEEE Trans. Signal Process.*, 2008, doi: 10.1109/TSP.2006.890827.
- [42] K. Maeda, H. Nakata, and K. Fujito, "Analysis of BER of 16QAM signal in AM/16QAM hybrid optical transmission system," *Electron. Lett.*, vol. 29, no. 7, pp. 640–642, 1993.
- [43] R. I. P, "RECOMMENDATION ITU-R P.372-9 Radio noise," Group, 2007.
- [44] V. Katkovnik, "New concept of adaptive beamforming for moving sources and

- impulse noise environment," *Signal Processing*, 2000, doi: 10.1016/S0165-1684(00)00094-3.
- [45] M. S. Lee, V. Katkovnik, and Y. H. Kim, "Robust approximate median beamforming for phased array radar with antenna switching," *Signal Processing*, 2004, doi: 10.1016/j.sigpro.2004.05.007.
- [46] H. Abu Hilal, "Error Rate Analysis of ZF and MMSE Decoders for Massive Multi Cell MIMO Systems in Impulsive Noise Channels," *Int. J. Wirel. Inf. Networks*, 2019, doi: 10.1007/s10776-019-00422-1.
- [47] F. H. JUWONO, R. REINE, and L. LIU, "Performance of impulsive noise blanking in precoded OFDM-based PLC systems," in *International Conference on Communication Systems (ICCS)*, 2016, pp. 1–6.
- [48] K. M. Rabie and E. Alsusa, "Performance analysis of adaptive hybrid nonlinear preprocessors for impulsive noise mitigation over power-line channels," in 2015 IEEE International Conference on Communications (ICC), Jun. 2015, pp. 728–733, doi: 10.1109/ICC.2015.7248408.
- [49] F. Sarabchi and C. Nerguizian, "Impulsive noise mitigation for OFDM-based systems using enhanced blanking nonlinearity," in 2014 IEEE 25th Annual International Symposium on Personal, Indoor, and Mobile Radio Communication (PIMRC), Sep. 2014, pp. 841–845, doi: 10.1109/PIMRC.2014.7136282.

- [50] L. Shhab, A. Rizaner, A. H. Ulusoy, and H. Amca, "Suppressing the effect of impulsive noise on millimeter-wave communications systems," *Radioengineering*, 2020, doi: 10.13164/RE.2020.0376.
- [51] H. Abu Hilal, "Neural networks applications for CDMA systems in non-Gaussian multi-path channels," *AEU Int. J. Electron. Commun.*, vol. 73, pp. 150–156, 2017, doi: 10.1016/j.aeue.2017.01.006.
- [52] R. Barazideh, S. Niknam, and B. Natarajan, "Impulsive noise detection in OFDM-based systems: A deep learning perspective," in 2019 IEEE 9th Annual Computing and Communication Workshop and Conference, CCWC 2019, Mar. 2019, pp. 937–942, doi: 10.1109/CCWC.2019.8666489.
- [53] O. Delgado and F. Labeau, "Deep Learning Decoder for MIMO Communications with Impulsive Noise," in 2020 IEEE 17th Annual Consumer Communications & Networking Conference (CCNC), Jan. 2020, pp. 1–6, doi: 10.1109/CCNC46108.2020.9045329.
- [54] A. M. Hmidat, B. S. Sharif, and W. L. Woo, "Fuzzy decorrelating detector for non-Gaussian CDMA channel," *Electron. Lett.*, 2004, doi: 10.1049/el:20040595.
- [55] A. H. Ulusoy and A. Rizaner, "Adaptive path selective fuzzy decorrelating detector under impulsive noise for multipath fading CDMA systems," *IEEE Commun. Lett.*, 2008, doi: 10.1109/LCOMM.2008.072012.

- [56] A. H. Ulusoy and A. Rizaner, "RBF network assisted adaptive path selective decorrelating detector under impulsive noise for multipath fading CDMA systems," *Ann. des Telecommun. Telecommun.*, 2011, doi: 10.1007/s12243-010-0212-0.
- [57] A. Alkhateeb, G. Leus, and R. W. Heath, "Limited Feedback Hybrid Precoding for Multi-User Millimeter Wave Systems," *IEEE Trans. Wirel. Commun.*, vol. 14, no. 11, pp. 6481–6494, 2015, doi: 10.1109/TWC.2015.2455980.
- [58] A. Alkhateeb, O. El Ayach, G. Leus, and R. W. Heath, "Channel estimation and hybrid precoding for millimeter wave cellular systems," *IEEE J. Sel. Top. Signal Process.*, vol. 8, no. 5, pp. 831–846, 2014, doi: 10.1109/JSTSP.2014.2334278.
- [59] D. Tse and V. Pramod, Fundamentals of wireless communication, vol.9780521845274. Cambridge University Press, 2005.
- [60] J. Brady, N. Behdad, and A. M. Sayeed, "Beamspace MIMO for millimeter-wave communications: System architecture, modeling, analysis, and measurements," *IEEE Trans. Antennas Propag.*, 2013, doi: 10.1109/TAP.2013.2254442.
- [61] W. U. Bajwa, J. Haupt, A. M. Sayeed, and R. Nowak, "Compressed channel sensing: A new approach to estimating sparse multipath channels," *Proc. IEEE*, 2010, doi: 10.1109/JPROC.2010.2042415.

- [62] A. M. Sayeed, "Deconstructing multiantenna fading channels," *IEEE Trans.*Signal Process., 2002, doi: 10.1109/TSP.2002.803324.
- [63] A. A. M. Saleh and R. A. Valenzuela, "A Statistical Model for Indoor Multipath Propagation," *IEEE J. Sel. Areas Commun.*, 1987, doi: 10.1109/JSAC.1987.1146527.
- [64] P. F. M. Smulders and L. M. Correia, "Characterisation of propagation in 60 GHz radio channels," *Electron. Commun. Eng. J.*, 1997, doi: 10.1049/ecej:19970204.
- [65] H. Xu, V. Kukshya, and T. S. Rappaport, "Spatial and temporal characteristics of 60-GHZ indoor channels," *IEEE J. Sel. Areas Commun.*, 2002, doi: 10.1109/49.995521.
- [66] V. Raghavan and A. M. Sayeed, "Sublinear capacity scaling laws for sparse MIMO channels," *IEEE Trans. Inf. Theory*, 2011, doi: 10.1109/TIT.2010.2090255.
- [67] L. Shhab, "Employing Preprocessor Filters to Suppress the Effect of Impulsive Noise on Communications Systems at Millimeter-Wave FrequenciesTitle," Eastern Mediterranean University, 2020.
- [68] R. Ziemer and W. Tranter, *Principles of Communications: Systems, Modulation and Noise*, 7th Editio. USA: John Wiley & Sons, Inc., 2015.

- [69] D. Middleton, "Canonical and Quasi-Canonical Probability Models of Class A Interference," *IEEE Trans. Electromagn. Compat.*, 1983, doi: 10.1109/TEMC.1983.304151.
- [70] D. Middleton, "Non-Gaussian noise models in signal processing for telecommunications: New methods and results for Class A and Class B noise models," *IEEE Trans. Inf. Theory*, 1999, doi: 10.1109/18.761256.
- [71] K. Gulati, A. Chopra, B. L. Evans, and K. R. Tinsley, "Statistical modeling of co-channel interference," in *GLOBECOM IEEE Global Telecommunications Conference*, 2009, pp. 1–6, doi: 10.1109/GLOCOM.2009.5425480.
- [72] B. L. Agba, F. Sacuto, M. Au, F. Labeau, and F. Gagnon, "Wireless Communications for Power Substations: RF Characterization and Modeling," Wireless Networks (United Kingdom), 2019.
- [73] D. W. J. Stein, "Detection of Random Signals in Gaussian Mixture Noise," *IEEE Trans. Inf. Theory*, 1995, doi: 10.1109/18.476307.
- [74] S. V. Vaseghi, Advanced Digital Signal Processing and Noise Reduction.Chichester, UK: John Wiley & Sons, Ltd, 2008.
- [75] M. Mulla, A. Rizaner, and A. H. Ulusoy, "Fuzzy Logic Based Decoder for Single-User Millimeter Wave Systems Under Impulsive Noise," *Wirel. Pers. Commun.*, 2021, doi: 10.1007/s11277-021-09435-7.

- [76] A. Goldsmith, S. A. Jafar, N. Jindal, and S. Vishwanath, "Capacity limits of MIMO channels," *IEEE J. Sel. Areas Commun.*, 2003, doi: 10.1109/JSAC.2003.810294.
- [77] S. Wang, M. He, J. Wang, R. Ran, H. Ji, and V. C. M. Leung, "A Family of Hybrid Precoding Schemes for Millimeter-Wave Massive MIMO Systems," *IEEE Syst. J.*, vol. 0, no. 0, pp. 1–11, 2022, doi: 10.1109/JSYST.2022.3147956.
- [78] Z. Wang, M. Li, Q. Liu, and A. L. Swindlehurst, "Hybrid Precoder and Combiner Design with Low-Resolution Phase Shifters in mmWave MIMO Systems," *IEEE J. Sel. Top. Signal Process.*, 2018, doi: 10.1109/JSTSP.2018.2819129.
- [79] P. Jain, P. Netrapalli, and S. Sanghavi, "Low-rank matrix completion using alternating minimization," in *Proceedings of the 45th annual ACM symposium on Symposium on theory of computing STOC '13*, 2013, p. 665, doi: 10.1145/2488608.2488693.
- [80] P. Netrapalli, P. Jain, and S. Sanghavi, "Phase Retrieval Using Alternating Minimization," *IEEE Trans. Signal Process.*, 2015, doi: 10.1109/TSP.2015.2448516.
- [81] Y. Wang, J. Yang, W. Yin, and Y. Zhang, "A new alternating minimization algorithm for total variation image reconstruction," *SIAM J. Imaging Sci.*, 2008, doi: 10.1137/080724265.

- [82] T. F. Chan and C. K. Wong, "Convergence of the alternating minimization algorithm for blind deconvolution," *Linear Algebra Appl.*, 2000, doi: 10.1016/S0024-3795(00)00141-5.
- [83] H. Kim and H. Park, "Nonnegative matrix factorization based on alternating nonnegativity constrained least squares and active set method," *SIAM J. Matrix Anal. Appl.*, 2008, doi: 10.1137/07069239X.
- [84] G. H. Golub and C. F. Van Loan, *Matrix Computations (4th Ed.)*. John Hopkins University Press, 2013.
- [85] S. Boyd and L. Vandenberghe, *Convex Optimization*. Cambridge: Cambridge University Press, 2004.
- [86] J. Nocedal and S. J. Wright, *Numerical Optimization*, 2nd Editio. Springer Verlag, 2006.
- [87] J. Frédéric Bonnans, J. Charles Gilbert, C. Lemaréchal, and C. A. Sagastizábal, Numerical optimization: Theoretical and practical aspects. Springer Berlin Heidelberg, 2006.
- [88] M. R. Hestenes and E. Stiefel, "Methods of conjugate gradients for solving linear systems," *J. Res. Natl. Bur. Stand.* (1934)., 1952, doi: 10.6028/jres.049.044.
- [89] B. Jiang and Y. H. Dai, "A framework of constraint preserving update schemes

- for optimization on Stiefel manifold," *Math. Program.*, vol. 153, no. 2, pp. 535–575, 2015, doi: 10.1007/s10107-014-0816-7.
- [90] Y. H. Dai and C. X. Kou, "A Barzilai-Borwein conjugate gradient method," *Sci. China Math.*, 2016, doi: 10.1007/s11425-016-0279-2.
- [91] Y. H. Dai, "A New Analysis on the Barzilai-Borwein Gradient Method," *J. Oper. Res. Soc. China*, vol. 1, no. 2, pp. 187–198, 2013, doi: 10.1007/s40305-013-0007-x.
- [92] Y. Xiao, H. Song, and Z. Wang, "A modified conjugate gradient algorithm with cyclic Barzilai-Borwein steplength for unconstrained optimization," *J. Comput. Appl. Math.*, vol. 236, no. 13, pp. 3101–3110, 2012, doi: 10.1016/j.cam.2012.01.032.
- [93] E. G. Birgin, J. M. Martínez, and M. Raydan, "Spectral projected gradient methods: Review and perspectives," *J. Stat. Softw.*, 2014, doi: 10.18637/jss.v060.i03.
- [94] M. Raydan, "On the barzilai and borwein choice of steplength for the gradient method," *IMA J. Numer. Anal.*, 1993, doi: 10.1093/imanum/13.3.321.
- [95] M. Raydan, "The Barzilaiai and Borwein gradient method for the large scale unconstrained minimization problem," *SIAM J. Optim.*, 1997, doi: 10.1137/S1052623494266365.

- [96] L. Grippo and M. Sciandrone, "Nonmonotone globalization techniques for the Barzilai-Borwein gradient method," *Comput. Optim. Appl.*, 2002, doi: 10.1023/A:1020587701058.
- [97] A. Hjorungnes, *Complex-Valued Matrix Derivatives*. Cambridge University Press, 2011.
- [98] R. Fletcher, *Practical Methods of Optimization*. John Wiley & Sons, Ltd, 2000.
- [99] T. Crosby, B. Iglewicz, and D. C. Hoaglin, "How to Detect and Handle Outliers," *Technometrics*, 1994, doi: 10.2307/1269377.
- [100] A. Rizaner, A. H. Ulusoy, and H. Amca, "Adaptive fuzzy assisted detector under impulsive noise for DVB-T systems," *Optik (Stuttg)*., vol. 127, no. 13, pp. 5196–5199, 2016, doi: 10.1016/j.ijleo.2016.02.079.
- [101] J. C. Chen, "Gradient Projection-Based Alternating Minimization Algorithm for Designing Hybrid Beamforming in Millimeter-Wave MIMO Systems," *IEEE Commun. Lett.*, 2019, doi: 10.1109/LCOMM.2018.2878712.
- [102] H. Yuan, J. An, N. Yang, K. Yang, and T. Q. Duong, "Low complexity hybrid precoding for multiuser millimeter wave systems over frequency selective channels," *IEEE Trans. Veh. Technol.*, vol. 68, no. 1, pp. 983–987, 2019, doi: 10.1109/TVT.2018.2880787.